

Neutron beta decay

J S Nico

National Institute of Standards and Technology, 100 Bureau Dr., Stop 8461, Gaithersburg, MD 20899, USA

E-mail: jnico@nist.gov

Received 24 March 2009

Published 16 September 2009

Online at stacks.iop.org/JPhysG/36/104001

Abstract

Studies of low-energy processes, such as neutron beta-decay, contribute important information regarding different aspects of physics including nuclear and particle physics and cosmology. The information from these systems is often complementary to that obtained from high-energy sources. Neutron decay is the most basic charged-current weak interaction in baryons. Precise measurement of the parameters characterizing it can be used to study the standard model as well set limits on possible extensions to it. This paper gives an overview of some of the basic features of neutron beta decay and summarizes the status of some recent developments.

(Some figures in this article are in colour only in the electronic version)

1. Introduction

Despite the success of the standard model (SM), it is widely thought to be incomplete and part of some larger description of the physical world. It does not contain gravity; it does not predict the masses of quarks and leptons or the coupling constants; and it does not explain the baryon asymmetry of the universe. One aim of experimental physics is to perform measurements in a variety of systems where one may find deviations from predictions of the SM or a new phenomenon that may provide theorists with additional clues to answer some of these questions. The neutron is one such system where one may test the robustness of the SM while probing for hints of new physics. These tests fall into the category of precision measurements, and in contrast to high-energy scale experiments, they may indicate a failure of the SM but do not directly specify the new physics.

Neutron beta decay is the process in which a neutron is transformed into a proton, electron and electron antineutrino. This process is well described by the charged weak current model [1–3] as a left-handed, purely $V-A$ interaction. Studying the rate at which this process occurs and the angular correlations among the decay products provides insight into this basic semileptonic decay. As the prototypical nuclear beta decay, it is sensitive to certain

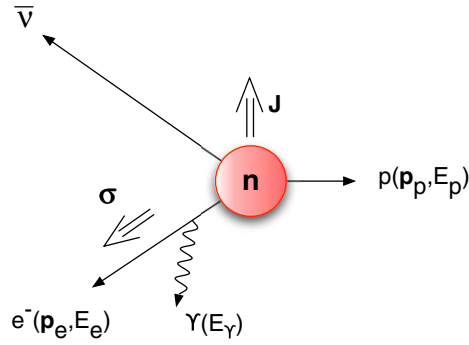


Figure 1. Decay of the neutron showing its currently accessible observables. E_i and \mathbf{p}_i are the energies and momenta, and \mathbf{J} and σ are the polarization of the neutron and electron, respectively. Other observable quantities are the angles among the spins and outgoing momenta.

SM extensions in the charged-current sector. Neutron decay can determine the Cabibbo–Kobayashi–Maskawa (CKM) matrix element V_{ud} through increasingly precise measurements of the neutron lifetime and the decay correlation coefficients.

Experiments in neutron decay test SM assumptions by measuring the lifetime and performing measurements on the many angular correlations of the decay products. These observables include the proton and electron energy and momentum, the electron spin, the neutron spin and the angles among the polarized particles, as depicted in figure 1. Direct detection of the antineutrino is not practical, but conservation of energy and momentum allows its kinematics to be inferred from the other decay products. The decay has sensitivity to possible right-handed currents, scalar and tensor terms in the weak interaction, and time-reversal violating correlations. Neutron decay is a good system in which to study discrete symmetries of nature. The symmetries of charge conjugation (\mathcal{C}), parity inversion (\mathcal{P}) and time invariance (\mathcal{T}) are of particular interest to theorists. Parity was found to be maximally violated in the weak interaction [4] through the investigation of decay correlations [5, 6]. Studies of \mathcal{CP} violation (and equivalently \mathcal{T} violation through the \mathcal{CPT} theorem) are possible because of angular correlations among the neutron decay products. To date, all experiments are consistent with the SM and the $V-A$ description of the weak interaction. Thus, owing to this success between experiment and theory, both are continually challenged to improve their precision because any such effects would reveal themselves only as very small deviations from the SM.

Within the SM, neutron decay is viewed more fundamentally as the conversion of a down quark into an up quark through the emission of a virtual W gauge boson. The reaction $d + \nu_e \leftrightarrow u + e^-$ is fundamental to a host of physical phenomena including primordial element abundance, solar burning and neutrino cross sections. Neutron decay influences the dynamics of big bang nucleosynthesis (BBN) through both the size of the weak interaction coupling constants and the lifetime. The couplings determine when weak interaction rates fall sufficiently below the Hubble expansion rate to cause neutrons and protons to fall out of chemical equilibrium. The neutron-to-proton ratio decreases as the neutrons decay, and it follows that the neutron lifetime determines the fraction of neutrons available for light element formation, primarily ${}^4\text{He}$ [7], as the universe cools. The value of the lifetime plays a critical role in the balance between protons and neutrons, and it remains the most uncertain nuclear parameter in cosmological models that predict the cosmic ${}^4\text{He}$ abundance [8, 9].

The physics that one may access using neutrons in contexts other than beta decay is extremely diverse and beyond the scope of this paper, which focuses on reviewing some of the physics that one addresses by observing the decay of the neutron. Section 1 gives some of the basic properties of the neutron and a brief digression on cold and ultracold neutrons, which are the sources for all modern experiments. Section 2 is an overview of the theoretical foundation of neutron beta decay. Strategies to measure the lifetime and the status of some experimental efforts are presented in section 3, and a similar treatment is given for correlation coefficients in section 4. Lastly, section 5 discusses recent efforts to look at other decay modes of the neutron.

The paper confines itself to the physics where experiments are currently accessible (or very nearly so), and more detailed considerations may be found in the references and many excellent reviews. Both theoretical and experimental activity in neutron physics have increased noticeably in recent years, and several reviews address the current state of many of these topics [10–15]. There are several textbooks that cover that breadth of neutron physics [16–19] and fundamentals of weak interaction theory [20–22]. In addition, the proceedings of recent international conferences also describe many experiments, measurements in progress and experimental concepts [23–26]. Finally, neutron decay is, of course, a subset of the larger class of beta decay. Much of the same physics is accessible by beta-decay experiments performed with nuclei, and discussions of those experiments may be found elsewhere [14, 27].

1.1. Basic physical properties

After the discovery of the neutron by Chadwick in 1932 [28], an experiment was performed by Chadwick and Goldhaber in which they irradiated deuterons with gamma radiation [29]. This irradiation caused the photo-disintegration of the deuteron into its constituent proton and neutron. By measuring the energy released in the reaction and knowing the masses of the deuteron and proton, they were able to estimate the mass of the neutron. The precision of the experiment was sufficient to determine that the mass of the neutron was greater than that of the proton. The implication of this discovery was that it is energetically allowed for the neutron to decay. Although it was more than a decade later before Snell and Miller first observed the decay of the neutron [30], the usefulness of neutron decay and beta decay in general, as a tool for studying the theory of the weak interaction was clear.

In 1930, Pauli proposed the existence of the neutrino to resolve the problem of the continuous energy distribution of electrons emitted in beta decay. With this postulated neutral and massless particle, Fermi was able to advance a theory of beta decay [31] using the weak interaction based on existing concepts of electrodynamics. Beta decay could be viewed as a four-fermion interaction $n \rightarrow e^- + p + \bar{\nu}_e$ where the vertex occurs at single point in spacetime, as illustrated in figure 2(a).

In leading recoil order, the total energy Q available for the decay is

$$Q = (m_n - m_p - m_{e^-})c^2 \approx 782 \text{ keV}. \quad (1)$$

The energy is distributed among the decay particles, and the properties of the particles largely drive the kinematics of the decay process. Figure 3 shows the kinetic-energy distribution for the three-body decay of the neutron. The mass difference between the neutron and proton is small, $(m_n - m_p)c^2 = 1.293 \text{ MeV}$, particularly in comparison with their masses which are of order 1 GeV. Because of the very small mass difference, the only possible decay channel available for W is the electron with its mass of $0.511 \text{ MeV}/c^2$. Two logical candidates, the pion ($M_{\pi^-} = 139.6 \text{ MeV}/c^2$) and muon ($M_{\mu^-} = 105.7 \text{ MeV}/c^2$), are energetically disallowed.

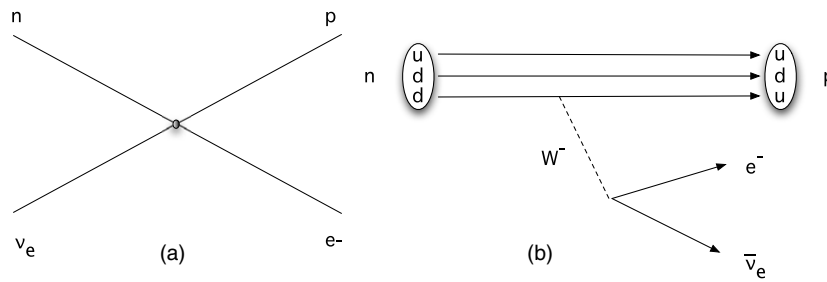


Figure 2. Neutron decay as (a) a Fermi four-point interaction and (b) at the quark level.

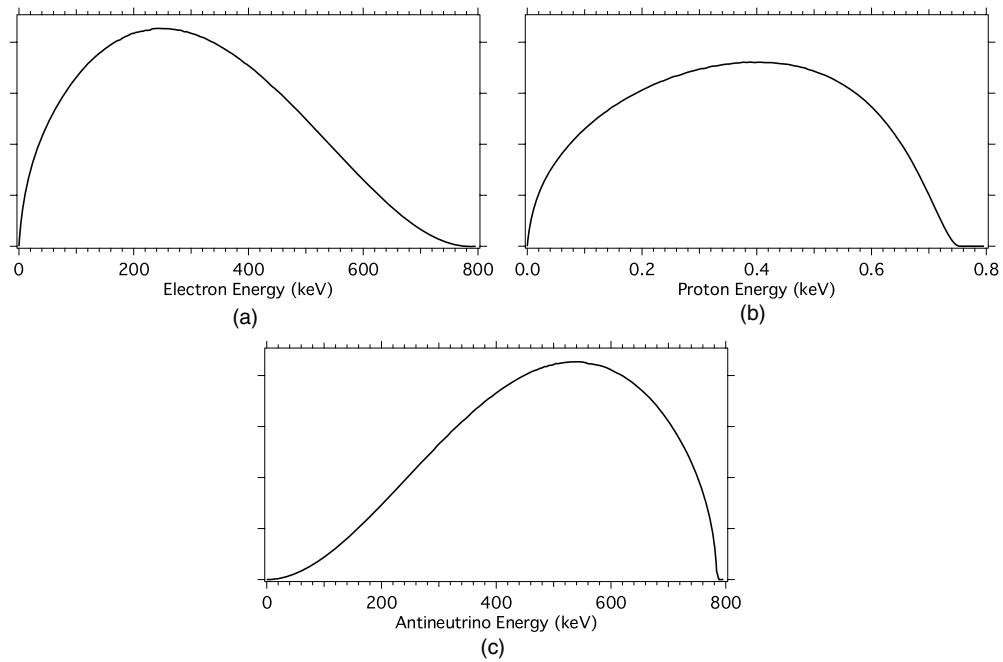


Figure 3. Spectra of the kinetic-energy distribution for the (a) electron, (b) proton and (c) antineutrino.

Another consequence of such a small mass difference is that it makes the recoil parameter of the decay small. The ratio of mass difference to the total mass gives an estimate of the recoil parameter of $\sim 10^{-3}$, and hence the momentum transfer is negligible. This leads to the unusually long lifetime of the neutron of about 15 min. (Consider the muon, more typically, where the recoil parameter is nearly unity and its lifetime is $2.2 \mu s$.) The neutron–proton mass difference is comparable to the binding energies within nuclei, and thus the energy available for decay (i.e., its lifetime) will depend significantly on the nuclear environment. Hence, a bound neutron can have a wide range of lifetimes, including being stable.

With the assumption that neutron decay is pointlike, there is no change in total orbital angular momentum, and one can consider the selection rules for allowed transitions between initial and final states. If the electron and antineutrino spin are aligned with total spin 0, then the proton must have the same spin as the neutron. A decay in which the change in spin and isospin is zero ($|\Delta J| = 0$ and $|\Delta I| = 0$) and there is no parity change is referred to as a Fermi

decay. If the electron and antineutrino spins are aligned with total spin 1, however, the proton couples to three possible spin states determined by Pauli spin matrices. These decays can change the spin and isospin by 0 or 1 ($|\Delta J| = 0, 1$ but with $J_i = 0 \rightarrow J_f = 0$ forbidden and $|\Delta I| = 0, 1$) and are known as Gamow–Teller decays. As all of these channels are available to the neutron, it is known as a mixed Fermi/Gamow–Teller transition.

One might think that the probabilities of these decays occur in the ratio of 3:1, but there is a small deviation that is a measure of the difference in the coupling strengths of the two decay channels. The ratio is instead parametrized by a factor such that $3\lambda^2:1$, where the value of λ is determined experimentally to be 1.2695 ± 0.0029 [32]. Physically, this difference in the coupling strength arises from nucleon structure effects, or in other words, the assumption that the decay constituents are pointlike is not precisely correct. The value of λ is a sensitive probe of the inner dynamics, and its study is one of the prime aims of beta-decay experiments.

1.2. Sources for neutron experiments

With such a long lifetime, neutrons must be produced in very large quantities in order to produce usable rates of decay particles. Experiments are therefore performed at facilities that are able to produce such quantities through either nuclear fission or spallation. In either case, neutrons are liberated from nuclei with MeV-scale energies and then moderated over many decades of energy to thermal energy and below. High-energy neutrons are not useful for beta-decay studies for many reasons, the two most obvious being that they are very difficult to collimate and with such large velocities very few decay within a detector.

The most intense sources of neutrons for experiments near thermal energies are nuclear reactors, and accelerators can produce higher energy neutrons by spallation. Both thermodynamic and optical language are frequently used to describe different energy regimes; for example, a neutron with a kinetic energy of 25 meV is also referred to as being at 300 K or having a de Broglie wavelength of 0.18 nm. Because a neutron's thermal wavelength is comparable to interatomic distances, this energy also represents the boundary below which coherent interactions of neutrons with matter become particularly important. This phenomenon is the reason for the existence of the field of neutron optics (for example, see [33]), and more directly, it permits the implementation of neutron guides that greatly enhance the number of neutrons available for experiments.

Modern experiments involving neutron decay use either beams of cold neutrons or ultracold neutrons (UCN) confined via materials, magnetic fields, gravity or some combination of the three. Cold neutron beams have energies between 0.05 meV and 25 meV, which are equivalent to temperatures from 0.6 K to 300 K or equivalently wavelengths of 4 nm to 0.18 nm. For a cold neutron beam or UCN, the momentum of the neutron is very small with respect to the decay proton ($|\mathbf{p}_n|/|\mathbf{p}_p| \sim 10^{-3}$), and for many classes of experiments the neutron may be considered to be at rest.

While neutron beams can be very intense in terms of the total fluence rate ($\sim 10^{10} \text{ cm}^{-2} \text{ s}^{-1}$), the long lifetime renders most of those neutrons unusable. It is one of several factors that make neutron-decay experiments difficult. The scale of the number of usable decays is set by the lifetime τ_n (≈ 900 s) and the observation time t in the factor e^{-t/τ_n} . For a typical neutron-decay experiment using a cold beam of average wavelength 0.5 nm, the observation time is about a millisecond, and thus the factor is of order 10^{-6} . The situation is even more difficult because those neutrons that do not decay may produce backgrounds. Neutron activation is a particularly pernicious problem. Beam neutrons may capture on the materials used in the construction of the apparatus, potentially creating large

amounts of radiation, particularly in comparison with the number of beta-decay events. Thus, experiments must be carefully designed to shield the detectors from these background sources.

In the neutron energy spectrum from a cold moderator, there is a very small fraction whose energies lie below the $\sim 10^{-7}$ eV neutron optical potential of matter. Such neutrons are called ultracold neutrons, and they can be trapped by total external reflection from material media. The existence of such neutrons was established experimentally in the late 1960s [34, 35]. By confining UCN within the experimental apparatus, one eliminates the biggest neutron loss mechanism of beams: namely, that of neutrons exiting the experiment before decaying. The cost, however, is the very low population of neutrons that exists far out on the low energy tail of the Maxwell–Boltzmann distribution of a cold moderator. Presently, cold beams produce significantly higher rates of neutron-decay events than the best UCN sources. Regardless, the highest decay rate within the apparatus may not be most important consideration, and UCNs may be preferable for systematic or technical reasons. In addition, new types of UCN converters have been developed that can increase the phase-space density through the use of ‘superthermal’ techniques [36]. They involve energy dissipation in the moderating medium (through phonon or magnon creation) and can therefore circumvent Liouville’s theorem and increase the phase-space density of the UCN. In effect, the bulk of the energy of the neutron is dissipated in the medium, and the resulting energy of the neutron is sufficiently low that it can be confined with magnetic fields via its interaction with the neutron magnetic moment. Superfluid helium [37] and solid deuterium [38] have been used most successfully as superthermal UCN sources, and other possible UCN moderating media, such as solid oxygen, are also being studied [39].

2. Overview of neutron beta decay

2.1. The lifetime

Our understanding of the neutron has improved tremendously through its description within the standard model. It is considered to be composed of two down quarks and an up quark, and it is stable under the strong and electromagnetic interactions. The weak interaction can convert a down quark into an up quark through the emission of a virtual W gauge boson (see figure 2(b)). In quantum mechanics, Fermi’s golden rule states that the transition rate (i.e., inverse of the lifetime τ) from an initial to final state is given by

$$W = \frac{2\pi}{\hbar} |\mathcal{M}|^2 \rho, \quad (2)$$

where $|\mathcal{M}|$ is a matrix element describing the interaction and ρ is the density of final states. That concept can be extended in field theory, and with an assumption that only vector and axial-vector currents are involved, one can construct a matrix element describing neutron decay in the standard model as a four-fermion interaction composed of hadronic and leptonic matrix elements. A current in the weak interaction may be described by

$$\frac{ig}{2\sqrt{2}} \bar{\psi}_1 \gamma_\mu (C_V + C_A \gamma_5) \psi_2, \quad (3)$$

where ψ_i are field operators and γ_μ are the gamma matrices. g is the weak coupling constant and, at level of fundamental fields, can be viewed analogously to the electric charge e in quantum electrodynamics. As noted, free neutron decay is well described by a mixed Fermi/Gamow–Teller transition; Fermi decays arise from vector currents while Gamow–Teller decays arise from axial-vector currents. The relative strengths of the two are characterized by two coupling strengths, C_V and C_A . These strengths are $C_V = +1$ and $C_A = -1$ for the weak

interaction in leptons, and it is assumed that $C'_V/C_V = C'_A/C_A = +1$. This is the origin of the description of the interaction as $V - A$ (vector minus axial vector) theory.

This is not the situation for hadrons where the strong interaction alters the decay of the d quark. For zero momentum transfer, the conserved-vector-current (CVC) hypothesis requires $C_V = +1$, but the axial vector coupling can be modified and need no longer be -1 . This factor is not known and must be determined empirically. There is one other factor that alters the hadronic portion of the interaction because the strong eigenstates are not exactly the weak eigenstates. The physical implication of this is that the coupling between the up (u) and down (d) quarks is weakened by a constant factor known as V_{ud} , the first element of the CKM matrix (discussed further in section 2.3). Because the momentum transfer is so small with respect to the mass of the W boson (M_W), the propagator can be represented by $g_{\mu\nu}/M_W^2$. Thus, one can write the decay matrix element for both the leptonic and hadronic matrix elements as

$$\mathcal{M} = \frac{i g}{2\sqrt{2}} V_{ud} \bar{\psi}_u \gamma_\mu (C_V + C_A \gamma_5) \psi_d \frac{g_{\mu\nu}}{M_W^2} \frac{i g}{2\sqrt{2}} \bar{\psi}_e \gamma^\mu (1 - \gamma_5) \psi_\nu, \quad (4)$$

where $\psi_{u,d,e,\nu}$ are the up, down, electron and antineutrino fermion fields. In low-energy limit W is subsumed into a constant defined as $\sqrt{2}g^2/(8M_W^2)$ and known as the Fermi coupling constant. It is experimentally determined from muon decay to be $G_F/(\hbar c)^3 = 1.16637(1) \times 10^{-5} \text{ GeV}^{-2}$ [32]. The weak coupling strengths can also be subsumed into two new constants $g_{V,A} \equiv C_{V,A}(q^2 \rightarrow 0) V_{ud} G_F$, and equation (4) can be written as

$$\mathcal{M} = i \bar{\psi}_p \gamma_\mu (g_V + g_A \gamma_5) \psi_n g_{\mu\nu} \bar{\psi}_e \gamma^\mu (1 - \gamma_5) \psi_\nu. \quad (5)$$

Using this matrix element, one can evaluate the neutron decay rate to be

$$W = \tau^{-1} = \frac{m_e^5 c^4}{2\pi^3 \hbar^7} |\mathcal{M}|^2 f, \quad (6)$$

where

$$f = \int_0^{E_0} F(Z, E'_e) p'_e E'_e (E_0 - E'_e)^2 dE'_e \quad (7)$$

is a phase-space statistical factor. Here p'_e and E'_e are the electron momentum and energy, respectively, and E_0 is the electron endpoint energy. The factor f includes a correction for the Coulomb attraction of the final states known as the Fermi function, $F(Z, E'_e)$. Physical constants have now been included. The leptonic portion of the matrix element can be calculated in a straightforward manner. The hadronic portion is composed of both the Fermi and Gamow–Teller contributions, and for the neutron integrating over their spin contributions gives $|\mathcal{M}^F|^2 = g_V^2$ and $|\mathcal{M}^{GT}|^2 = 3g_A^2$. The total lifetime can be expressed as

$$\tau^{-1} = \frac{m_e^5 c^4}{2\pi^3 \hbar^7} (g_V^2 + 3g_A^2) f. \quad (8)$$

Thus far, radiative corrections have not been considered, but for the neutron they come predominantly as δ_R , the so-called nucleus-dependent radiative correction that modifies f such that $f(1 + \delta_R)$, and Δ_R^V , the nucleus-independent correction. The correction Δ_R^V is common to all beta decays [40] and takes $g_V^2 \rightarrow g_V^2(1 + \Delta_R^V)$. Finally, one can write an expression for V_{ud} in terms of the neutron lifetime with its radiative corrections as

$$|V_{ud}|^2 = \frac{1}{f(1 + \delta_R) \tau_n} \frac{K}{G_F^2(1 + \Delta_R^V)(1 + 3\lambda^2)}, \quad (9)$$

where $f(1 + \delta_R) = 1.71489 \pm 0.00002$ [41], K is a constant equal to $2\pi^3 \hbar^7 / (m_e^5 c^4)$ and Δ_R^V is the nucleus-independent radiative correction [42]. Equation (9) indicates that two observables are necessary to extract V_{ud} : the ratio of the two coupling constants

$\lambda \equiv |g_A/g_V| e^{i\phi} = -1.2695 \pm 0.0029$ (where ϕ allows for a phase between the two couplings) and the lifetime $\tau_n = (885.7 \pm 0.8)$ s [32].

Improved calculations of the radiative corrections in equation (9) were recently performed yielding

$$|V_{ud}|^2 = \frac{(4908.7 \pm 1.9)\text{s}}{\tau_n(1 + 3\lambda^2)}. \quad (10)$$

The new method for calculating hadronic corrections to weak radiative corrections combines high-order perturbative QCD calculations with a large N -based extrapolation; it has also been applied to superallowed nuclear beta decay [43]. This calculation reduced the theoretical loop uncertainty by approximately a factor of 2. The relative uncertainty in the theoretical corrections is only 0.4%, less than the present experimental uncertainty of 0.9%.

2.2. Correlation coefficients

In the discussion of the lifetime, the matrix element of equation (3) assumed that the couplings were purely vector and axial vector. It is important to emphasize that this is not the most general interaction Hamiltonian that one can construct. In 1956, Lee and Yang parametrized the interaction in terms of the coupling constants C_i and C'_i that describe the strength of the nucleon interactions [4]. In addition to V and A currents, they allowed the possibility of scalar (S), tensor (T) and pseudoscalar (P) currents. It yields ten possible couplings under the assumption that all are real and 20 couplings if each is allowed an imaginary component (i.e., \mathcal{T} may be violated). The charged weak current theory has been remarkably successful in describing the interaction with only the two real couplings, C_A and C_V . It restricts the weak interaction to operate only on the left-handed components of the quark and lepton fields, but a more fundamental understanding of the reason for this parity-odd structure of the weak interaction is still lacking. It has motivated numerous experimental efforts to look for evidence of additional interactions to help provide a deeper understanding.

Using the more general interaction Hamiltonian, the probability distribution for beta decay in terms of the nucleus spin and the energies and momenta of the decay products was worked out in detail in 1957 by Jackson *et al* [44]. They considered the large number of correlations that exist when considering the polarization states of the nucleus and its decay particles. The angular distribution of the decay particles from a polarized nucleus can be written as

$$W(\langle \mathbf{J} \rangle, E_e, \Omega_e, \Omega_\nu) dE_e d\Omega_e d\Omega_\nu = \frac{1}{(2\pi)^5} p_e E_e (E^0 - E_e)^2 dE_e d\Omega_e d\Omega_\nu \\ \times \xi \left[1 + a \frac{\mathbf{p}_e \cdot \mathbf{p}_\nu}{E_e E_\nu} + b \frac{m_e}{E_e} + \frac{\langle \mathbf{J} \rangle}{J} \cdot \left(A \frac{\mathbf{p}_e}{E_e} + B \frac{\mathbf{p}_\nu}{E_\nu} + D \frac{\mathbf{p}_e \times \mathbf{p}_\nu}{E_e E_\nu} \right) \right]. \quad (11)$$

In this equation, \mathbf{p}_e , \mathbf{p}_ν , E_e and E_ν are the momenta and kinetic energies of the decay electron and antineutrino and $\langle \mathbf{J} \rangle / J$ is nuclear polarization (see figure 1). The dimensionless factors in front of each term are referred to as correlation coefficients, and they parametrize the relationship among the decay particles in equation (11). The factor ξ is most generally given by

$$\xi = |\mathcal{M}_F|^2 (|C_S|^2 + |C_V|^2 + |C'_S|^2 + |C'_V|^2) + |\mathcal{M}_{GT}|^2 (|C_T|^2 + |C_A|^2 + |C'_T|^2 + |C'_A|^2). \quad (12)$$

Note in $V - A$ theory this factor for the neutron reduces to the familiar expression $(g_V^2 + 3g_A^2)$.

Table 1. Beta-decay correlations where there are existing measurements or active experimental efforts involving the neutron. The first column gives the coefficient with its common name. The second column gives the expression for the correlation. The last two columns give the behavior of correlation under the operation of \mathcal{P} and \mathcal{T} .

Coefficient	Correlation	Parity (\mathcal{P})	Time (\mathcal{T})
a (Electron–antineutrino correlation)	$\mathbf{p}_e \cdot \mathbf{p}_\nu / E_e E_\nu$	Even	Even
b (Fierz interference)	m_e / E_e	Even	Even
A (Spin–electron asymmetry)	$\langle \mathbf{J} \rangle \cdot \mathbf{p}_e / E_e$	Odd	Even
B (Spin–antineutrino asymmetry)	$\langle \mathbf{J} \rangle \cdot \mathbf{p}_\nu / E_\nu$	Odd	Even
C (Spin–proton asymmetry)	$\langle \mathbf{J} \rangle \cdot \mathbf{p}_p / E_p$	Odd	Even
D (Triple correlation)	$\langle \mathbf{J} \rangle \cdot (\mathbf{p}_e \times \mathbf{p}_\nu) / E_e E_\nu$	Even	Odd
N (Spin–electron spin)	$\boldsymbol{\sigma} \cdot \langle \mathbf{J} \rangle$	Even	Even
R (Electron spin triple correlation)	$\boldsymbol{\sigma} \cdot (\langle \mathbf{J} \rangle \times \mathbf{p}_e) / E_e$	Odd	Odd

Also considered in [44] is the decay of polarized nuclei and its correlations with the electron momentum and polarization $\boldsymbol{\sigma}$

$$\begin{aligned}
 W(\langle \mathbf{J} \rangle, \boldsymbol{\sigma}, E_e, \Omega_e) dE_e d\Omega_e &= \frac{1}{(2\pi)^4} p_e E_e (E^0 - E_e)^2 dE_e d\Omega_e \\
 &\times \xi \left[1 + \boldsymbol{\sigma} \cdot \left(N \frac{\langle \mathbf{J} \rangle}{J} + R \frac{\langle \mathbf{J} \rangle}{J} \times \frac{\mathbf{p}_e}{E_e} + \dots \right) + \dots \right], \tag{13}
 \end{aligned}$$

where N and R are correlations involving measurement of the electron polarization. Here the neutrino momentum was averaged over. Table 1 gives some information for correlation coefficients for which there are existing measurements or active experimental efforts.

Equations (11) and (13) describe nuclear beta decay in general. For the case of the neutron, if one assumes vector and axial-vector interactions but permits the possibility of time-reversal violation, the correlation coefficients may be expressed in terms of the weak coupling constants g_A and g_V and ϕ the phase angle between them, as in table 2. The parameter λ can be extracted from several of the correlations, but presently only measurements of A have sufficient precision to have an impact. If the neutron lifetime τ_n is also measured, g_V and g_A can be determined uniquely under the assumption that $\sin \phi = 0$. Radiative corrections to the correlation coefficients have been evaluated recently using several techniques [45–49]. The experiments discussed in section 4 proceed with the purposes of checking the corrections and testing the validity of these assumptions underlying the $V - A$ theory.

2.3. Testing CKM unitarity

Accurate determination of the parameters that describe neutron decay provides information regarding the completeness of the three-family picture of the SM through a test of the unitarity of the CKM matrix. The matrix represents a rotation of the quark mass eigenstates to the weak eigenstates

$$\begin{pmatrix} d_W \\ s_W \\ b_W \end{pmatrix} = \begin{pmatrix} V_{ud} & V_{us} & V_{ub} \\ V_{cd} & V_{cs} & V_{cb} \\ V_{td} & V_{ts} & V_{tb} \end{pmatrix} \begin{pmatrix} d \\ s \\ b \end{pmatrix}. \tag{14}$$

It arises because the weak eigenstates are presumed to be different from the mass eigenstates of electromagnetic and strong interactions [51, 52]. There is no physical understanding for

Table 2. The first two columns are the coefficients and their expressions in terms of the weak coupling constants and phase angle. For the spin-proton asymmetry, x_C is a calculated kinematic factor. The experimental values are given in the third column; they come from the 2008 PDG compilation [32] with the exception of N and R that are new measurements [50]. The fourth column gives the relative uncertainty. The last column is sensitivity of the correlation to λ and is defined as $|\frac{d_x}{\lambda}|/|\frac{d_x}{x}|$, where x is a given correlation coefficient. It is the factor that one multiplies the relative uncertainty in a correlation coefficient to obtain the relative uncertainty in λ .

Correlation coefficient	Expression	Experimental value	Relative uncertainty	λ Sensitivity
a	$\frac{1- \lambda ^2}{1+3 \lambda ^2}$	-0.103 ± 0.004	0.039	0.28
b	0			
A	$-2 \frac{ \lambda ^2 + \lambda \cos \phi}{1+3 \lambda ^2}$	-0.1173 ± 0.0013	0.011	0.25
B	$2 \frac{ \lambda ^2 - \lambda \cos \phi}{1+3 \lambda ^2}$	0.9807 ± 0.0030	0.003	10.2
C	$4x_C \frac{ \lambda \cos \phi}{1+3 \lambda ^2}$	-0.2377 ± 0.0026	0.011	1.5
D	$2 \frac{ \lambda \sin \phi}{1+3 \lambda ^2}$	$(-4 \pm 6) \times 10^{-4}$		
N	$2 \frac{m}{E} \frac{ \lambda ^2 + \lambda \cos \phi}{1+3 \lambda ^2}$	0.056 ± 0.012	0.21	0.25
R	0	0.008 ± 0.016		

the measured values of the CKM mixing matrix elements between the quark mass eigenstates and their weak interaction eigenstates. The fact that the matrix is unitary is ultimately a consequence of the universality of the weak interaction gauge theory; non-unitarity could also be an indication of a fourth generation of quarks. Extensions to the SM, which either introduce non- $V - A$ weak interactions or generate violations of universality, can therefore be tested through precision measurements in beta decay.

Unitarity of the first row of the CKM matrix requires $|V_{ud}|^2 + |V_{us}|^2 + |V_{ub}|^2 = 1$. The matrix elements $|V_{us}|$ and $|V_{ub}|$ are obtained from high-energy accelerator experiments. The CVC hypothesis states that $g_V = G_F |V_{ud}| (1 + \Delta_R^V)$, and thus one can determine $|V_{ud}|$ by measuring the transition strengths of superallowed $0^+ \rightarrow 0^+$ nuclear beta decays between isobaric analog states. All such decays should yield the same value for g_V from their measured ft values after nuclear structure effects and isospin breaking and radiative corrections are applied. A recent calculation of those contributions produces

$$|V_{ud}|^2 = \frac{(2984.48 \pm 0.05)s}{ft(1 + RC)}, \quad (15)$$

where RC is all of the correction contributions [43]. Using the nine best values of ft [53] gives $|V_{ud}| = 0.97418 \pm 0.00027$ [32]. Taking the PDG 2008 recommendations of $|V_{us}| = 0.2255 \pm 0.0019$ and $|V_{ub}| = (3.93 \pm 0.36) \times 10^{-3}$ yields

$$\sum_{i=d,s,b} |V_{ui}|^2 = 0.9999 \pm 0.0010. \quad (16)$$

This is the most precise method of determining $|V_{ud}|$ and the agreement with the SM is very good. There was a significant change in the value of $|V_{us}|$ that removed an approximately two-sigma discrepancy that had existed between the nuclear decays and the CKM unitarity requirement. The new result is based on recent experiments in semileptonic kaon decays, including measurements of the branching ratios, form factors and lifetime [54]. There are also renewed theoretical investigations to extract $|V_{us}|$ from hyperon decay [55] and precision

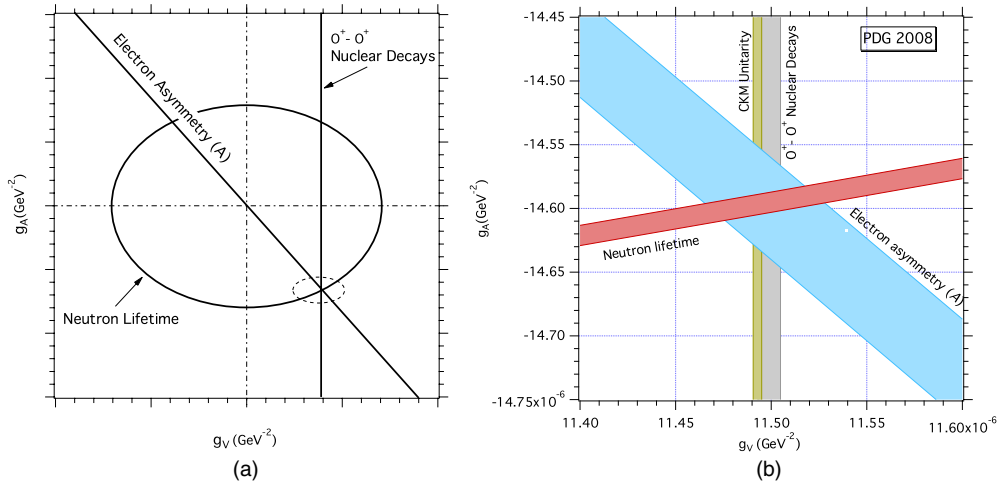


Figure 4. (a) Plot showing the functional dependence of the lifetime, λ , and the superallowed $0^+ \rightarrow 0^+$ nuclear decays on g_A and g_V . The dashed ellipse is expanded in the adjacent plot. (b) The weak coupling constants g_V and g_A determined from neutron-decay parameters and superallowed $0^+ \rightarrow 0^+$ nuclear decay transitions. The bands represent ± 1 standard deviation uncertainties including experimental and calculational uncertainties. For the decay parameters, the uncertainties are dominated by experimental uncertainties. For the superallowed $0^+ \rightarrow 0^+$ nuclear decays, the uncertainty is dominated by radiative correction calculations.

experiments in hadronic tau decays [56]. Extracting V_{us} requires a calculation of the form factor $f_+(0)$. The factor used in the PDG evaluation is calculated by Leutwyler and Roos [57] using chiral perturbation theory, but calculations employing other techniques [58] produce results that differ by as much as 2%. The value of $|V_{ub}|$ has also changed slightly, but it has a negligible contribution to the unitarity sum. The dominant uncertainty in the unitarity comparison comes from the calculation of the nucleus-dependent radiative corrections.

In neutron decay, the functional dependence of the two parameters on g_A and g_V is illustrated in figure 4(a) along with g_V from the superallowed nuclear decays. Equation (8) indicates that the lifetime forms an ellipse in g_A and g_V , and by definition, λ has linear relationship with g_A and g_V ; for superallowed decays only g_V enters at the tree level. While several of the correlation coefficients give λ , the most precise value comes from the spin-electron asymmetry A . With the PDG values for λ and τ_n , one obtains a value $|V_{ud}| = 0.9746 \pm 0.0019$. Figure 4(b) expands on intersection of the three experimental limits to elucidate the comparison with the superallowed decays.

A recent analysis was performed to extract λ that did not limit itself to experiments included in the PDG compilation. Using a larger data set of 25 independent experiments, including measurements of τ_n , a and B , they performed a least-squares fit with only one free parameter to extract $\lambda = C_A/C_V = -1.26992 \pm 0.00069$ [14]. The value is in good agreement with the PDG value but the uncertainty is about a factor of 4 smaller. Because the uncertainty in $|V_{ud}|$ from the neutron is dominated by λ , the corresponding uncertainty becomes significantly smaller, $|V_{ud}| = 0.97433 \pm 0.00065$. The central value is still in good agreement that from the superallowed nuclear decays but with a much reduced uncertainty.

It is also possible to extract $|V_{ud}|$ from pion beta decay in the pure vector transition $\pi^+ \rightarrow \pi^0 + e^+ + \nu_e$ in a manner that is free from structure-dependent corrections [59]. The PIBETA collaboration quotes a value of $|V_{ud}| = 0.9728 \pm 0.0030$ [59]. Pion beta decay is theoretically the cleanest system in which to measure $|V_{ud}|$, but the small branching ratio

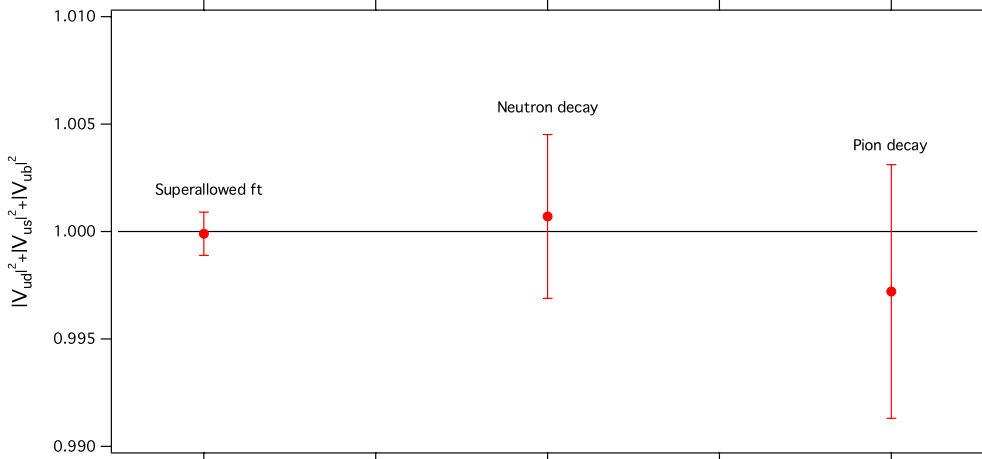


Figure 5. Plot showing CKM unitarity from superallowed nuclear decay, neutron decay and pion decay. The inputs come from the PDG 2008 compilation.

($\mathcal{O}(10^{-8})$) has so far precluded a measurement with enough sensitivity to compete with the superallowed beta decays.

Figure 5 shows the very good agreement in the comparison of CKM unitarity for the three systems, and the dominance of the superallowed nuclear decays in making that test. It represents a significant accomplishment in testing the SM. The array of experimental values that go into the determination of ft has proven very robust and has yielded a value for $|V_{ud}|$ that is limited by theoretical uncertainties. It has produced strong limits on additional weak interactions ($|C_S/C_V| < 0.0013$) and verified the CVC hypothesis at the level 0.026% [60]. Improvement in these limits is still possible through both new experimental efforts and calculations [53].

Despite the strong agreement, there are underlying assumptions not elucidated in figure 5. The neutron data are not yet competitive in determining $|V_{ud}|$, where the experimental uncertainties are about a factor of 7 times larger than those of the superallowed nuclear decays. Because of the intrinsically smaller corrections, the neutron is very promising avenue for investigation, but it must first resolve some disagreements. The consistency among four electron asymmetry experiments that are used in the PDG determination of λ is not good, and the PDG chose to increase the uncertainty by a scale factor of 2.0. In addition, the most precise measurement of the neutron lifetime is 6.5 standard deviations away from the PDG average and currently not included in the average. While it might be tempting to dismiss the measurement because of such a large disagreement with the other experiments and the poor effect it would have on the CKM unitarity comparison, one notes that this neutron lifetime value taken with the most precise measurement of the electron asymmetry again restores CKM unitarity. Clearly this situation is not satisfactory and must be clarified, and the prospects for doing so are promising. The situation with these experiments is discussed in greater detail in sections 3 and 4.1.

2.4. T -violation in Neutron beta decay

For more than 35 years, neutral kaons were the only system in which CP violation was observed [61]. More recent experiments have reported measuring CP violation in the $K^0 \rightarrow 2\pi$ amplitudes [62, 63] and in the decays of the neutral B-mesons [64, 65]. To date there is

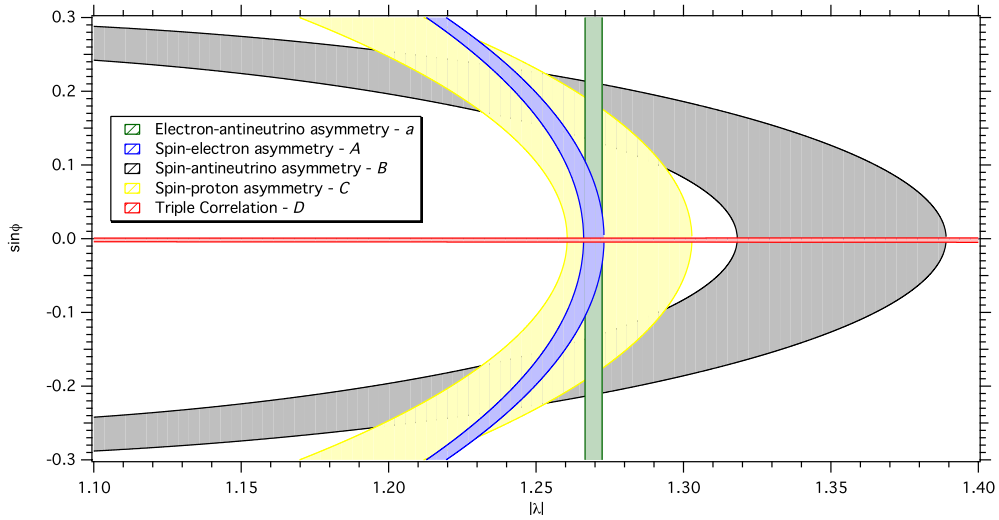


Figure 6. Plot of the experimental limits on the dependence of $\sin \phi$ on $|\lambda|$ [74]. In addition to showing the sensitivity of D , it illustrates the determinations of $|\lambda|$ from the correlation coefficients a , A , B and C . The bands are based on one-sigma uncertainties from the PDG [32].

no firm evidence against the possibility that the observed CP -violation effects are due to the Kobayashi–Maskawa phase δ_{KM} in the standard model [66]. A major question is whether or not there are sources of CP -violation other than δ_{KM} . One notes that δ_{KM} is not sufficient to generate the baryon asymmetry of the universe [67]. The most suitable observables to probe the existence of new CP -violation interactions are those for which the contribution from δ_{KM} is small. Examples of observables of this kind are the T -odd correlations in leptonic and semileptonic decays and electric dipole moments of the neutron and atoms. Decay correlations are not truly T odd as there are final-state interactions that produce correlations unrelated to time-reversal invariance, but these contributions have been calculated and are below the current levels of experimental sensitivity. Thus, with its small SM values of T -odd observables, neutron beta decay provides another excellent arena in which to search for time-symmetry violation.

2.4.1. D -coefficient. One correlation from equation (11) for polarized neutron decay is the triple correlation $D(\langle \mathbf{J} \rangle / J) \cdot (\mathbf{p}_e \times \mathbf{p}_\nu)$. The D coefficient is sensitive only to T -odd interactions with vector and axial vector currents, and the coefficients of the correlations depend on the magnitude and phase of $\lambda = |\lambda| e^{-i\phi}$. T invariance requires ϕ to be 0° or 180° , and the present value is $\phi = 180.06^\circ \pm 0.07^\circ$ [32]. Correlations from table 2 are in general a function of the phase ϕ , but D is sensitive to the imaginary part. Figure 6 illustrates the comparison of the sensitivities of some correlations to $\sin \phi$.

A neutron EDM would violate both T and \mathcal{P} symmetries, whereas a D -coefficient violates T but conserves \mathcal{P} . This makes the two classes of experiments sensitive to different SM extensions. Although constraints on T -violating, \mathcal{P} -conserving interactions can be derived from EDM measurements, these constraints may be model dependent [68, 69]. EDM and neutron-decay searches for T violation can be viewed as complementary. Leptoquark, left–right symmetric models, and exotic-fermion models can all lead to violations of time-reversal symmetry at potentially measurable levels. Recent work summarizes the current constraints on D from analyses of data on other T -odd observables for the SM and some extensions

[66, 70]. An investigation of D in the minimal supersymmetric standard model concluded that 10^{-7} is the maximum of the range permitted by the theory [71], a value almost four orders of magnitude beyond the current experimental limit.

Within the $V - A$ model, it is important to note that there are \mathcal{T} -conserving electromagnetic final-state interactions, such as Coulomb and weak magnetism scattering, that give rise to a non-zero triple correlation. The Coulomb term vanishes in $V - A$ theory in the limit of infinite nucleon mass [44], but in principle scalar and tensor interactions could contribute. Fierz interference coefficient measurements [60] can be used to limit this possible contribution to $|D^{EM}| < (1.0 \times 10^{-5}) \frac{m_e}{p_e}$. Interference between Coulomb scattering amplitudes and the weak magnetism amplitudes produces a final-state effect of order $\alpha E_e/m_n$. The magnitude of the final-state interaction, including weak magnetism and the contribution from the magnetic moment of the proton, is predicted to be $|D^{\text{fsi}}| \approx (0.23 p_e^{\text{max}}/p_e + 1.08 p_e/p_e^{\text{max}}) \times 10^{-5}$ [21, 72]. A recent calculation of this final-state interaction using heavy-baryon effective field theory has reproduced this result together with the dominant correction [73]. This is an important conclusion because the implication is that one should be able to measure D without theoretical ambiguities down to the level of $\sim 10^{-7}$.

Included for completeness, there exists another \mathcal{T} -odd, \mathcal{P} -even correlation that requires measuring the electron momentum and polarization as well as the recoil momentum

$$L\sigma \cdot \left(\frac{\mathbf{p}_e \times \mathbf{p}_\nu}{E_e E_\nu} \right). \quad (17)$$

There have been no efforts to measure this correlation. Roughly speaking, an experiment to measure L would be similar to a D experiment where one measures the electron polarization instead of the neutron polarization. While it is feasible to do so, the greater ease of performing neutron polarimetry has undoubtedly served to focus more experiments on D .

2.4.2. R -correlation. The expression for the D -coefficient in equation (11) integrates over all final spin states. For an experiment capable of measuring the electron polarization, equation (13) describes the distribution in the electron energy, angle and polarization for the decay of a polarized neutron. The R -correlation is given by

$$R\sigma \cdot \left(\frac{\langle \mathbf{J} \rangle}{J} \times \frac{\mathbf{p}_e}{E_e} \right). \quad (18)$$

The D - and R -correlations have different sensitivities to both \mathcal{T} violation and non-SM physics. While both are \mathcal{T} -odd, D is \mathcal{P} -even and R is \mathcal{P} -odd. The D -correlation is sensitive primarily to the imaginary part of the $V - A$ interference, and R has sensitivity to both scalar and tensor couplings. R vanishes in $V - A$ theory, independent of the phase of g_A and g_V . Recently the first experiment limiting R in neutron decay was performed [50], but the best limits on testing \mathcal{T} -invariance in the scalar and tensor weak interaction still come from nuclear decays [75, 76]. Figure 7 shows the limits on scalar and tensor currents from all sources. Measurement of the Gamow–Teller decay of ${}^8\text{Li}$ yielded $R = (0.9 \pm 2.2) \times 10^{-3}$, which sets the most stringent limits for time-reversal violating tensor couplings in semileptonic weak decays, $-0.022 < \text{Im}(C_T + C_T')/C_A < 0.017$ [77].

3. The neutron lifetime

3.1. Lifetime techniques

The neutron lifetime is governed by the exponential decay law $N(t) = N_0 e^{-t/\tau}$, where an initial population of particles N_0 is reduced to $N(t)$ at a rate determined by the lifetime τ . In comparison with other unstable particles, the approaches to measuring the neutron lifetime are

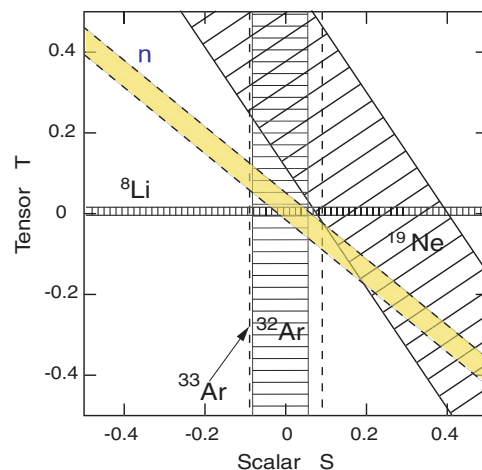


Figure 7. One-sigma limits from experiments testing the scalar and tensor interactions. The constraint from the measurement of the R -correlation in neutron decay is the statistical uncertainty only. Including (additively) systematics would broaden the yellow band by a third. Plot courtesy of K Bodek.

not typical. The usual approach forms a histogram of decay times relative to an initial time, and the lifetime is obtained in a straightforward manner from an exponential fit. This strategy only works, however, when one is able to define that initial time, which is very difficult with neutron beams and low-density, confined ultracold neutrons. In fact, it has been difficult to measure the neutron lifetime because of its unusually long lifetime, its neutrality and the difficulty in obtaining sufficiently dense populations that are not lossy. Several techniques have been pioneered to overcome the difficulties. Only recent experiments are presented here, but a discussion of previous experiments and their development is found elsewhere [78].

3.2. Beam technique

The exponential decay law can be rewritten in the differential form $dN(t)/dt = -N(t)/\tau$. One extracts the lifetime by measuring simultaneously both the average number of neutrons $N(t)$ in a well-defined fiducial volume of the beam and the rate of neutron decays dN/dt . Practically speaking, this entails measuring the absolute rate of neutrons traversing a known volume and the decay protons (or electrons) generated within the same volume. The first neutron lifetime measurements were performed with thermal beams using this method.

One potential difficulty is that the number of neutrons decaying within the volume will depend on the velocity (v) of the neutron while the number of total neutrons in the beam will be independent of the velocity. Correcting for this effect would be extremely difficult because it requires knowledge of the energy distribution of the neutrons in the beam, something that is very difficult to measure precisely. Fortunately, this problem can be avoided by using a neutron detector that has a $1/v$ dependence, which is exactly the same dependence for the rate of protons being produced within the volume. The measurement becomes independent of energy.

A significant improvement in the precision was obtained by implementing a segmented proton trap to better define the fiducial volume [79, 80]. Figure 8 shows a schematic illustration of the first such experiment. A highly collimated neutron beam enters a well-defined trapping

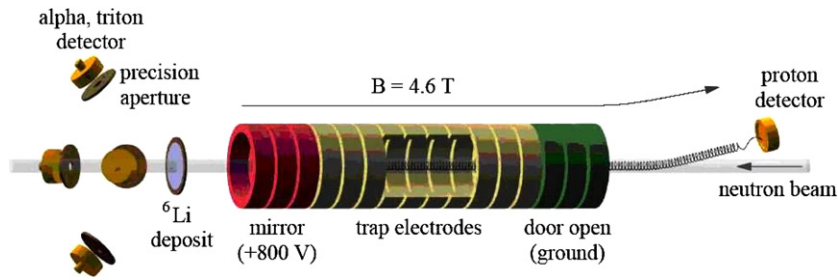


Figure 8. A schematic illustration of a neutron lifetime experiment using a cold neutron beam [81]. The highly collimated neutron beam enters a well-defined proton trapping volume. The trap is periodically opened and decay protons are guided to a detector. A neutron detector with an efficiency inversely proportional to the neutron velocity continuously monitors the neutron rate.

volume where a small number of the neutrons decay. The protons are confined by an axial magnetic field and electrostatic fields at each end. The trap can be periodically opened by lowering the voltage on one set of trap electrodes, and the protons are guided to a detector away from the beam. The neutron flux is continuously monitored during this process by a detector that has a response proportional to $1/v$ of the neutron velocity, thus eliminating $1/v$ dependence of the lifetime on the trapping volume.

The largest experimental challenge for this technique is that it requires absolute counting: one has to account for all the neutrons and protons. Even though the neutron counting rate is much higher than the proton counting rate, the precision of the beam experiments is limited by systematic effects related to neutron counting. The absolute efficiency of the best neutron monitors depends on cross sections and mass densities that are only known at approximately the 0.25% level. Regardless, efforts are in progress to calibrate these detectors, which would allow an improvement of the precision of the beam technique at the 1 s level.

3.3. Confined ultracold neutrons

An important new approach to measuring the lifetime was introduced with the advent of ultracold neutrons, neutrons with energies of about 100 neV. This energy is the size of typical optical potentials of matter and also the interaction of a neutron in the magnetic field on the order of a tesla. This fact allows the neutrons to be manipulated through interactions with both materials and magnetic fields. With the implementation of UCN production techniques, experimenters were able to confine neutrons in material ‘bottles’ or magnetic fields, as shown in figure 9. The lifetime can be extracted measuring the neutron population at two times, or $\tau_n = (t_2 - t_1) / \ln(N(t_1)/N(t_2))$. With this method one avoids the necessity of knowing the absolute neutron density and detector efficiencies, but naturally other systematic effects arise.

The lifetime that one measures is not the neutron lifetime because there are other mechanisms through which neutrons can be removed from the confinement volume other than decay. The measured lifetime is given by $\tau_{\text{tot}}^{-1} = \tau_n^{-1} + \tau_{\text{loss}}^{-1}$ and includes losses from the confinement cavity as well as neutron decay. To isolate τ_{loss} , which is typically dominated by nonspecular processes in the neutron interaction with the walls of the confinement vessel, one measures the lifetime in bottles with different surface-to-volume ratios and performs an extrapolation to an infinite volume (or equivalently, zero collision rate). These losses depend on the UCN energy spectrum, which can change during the storage interval, so much work has been done to understand the spectrum evolution and loss mechanisms and to find surface materials with lower loss probabilities. To address losses experimentally, one group

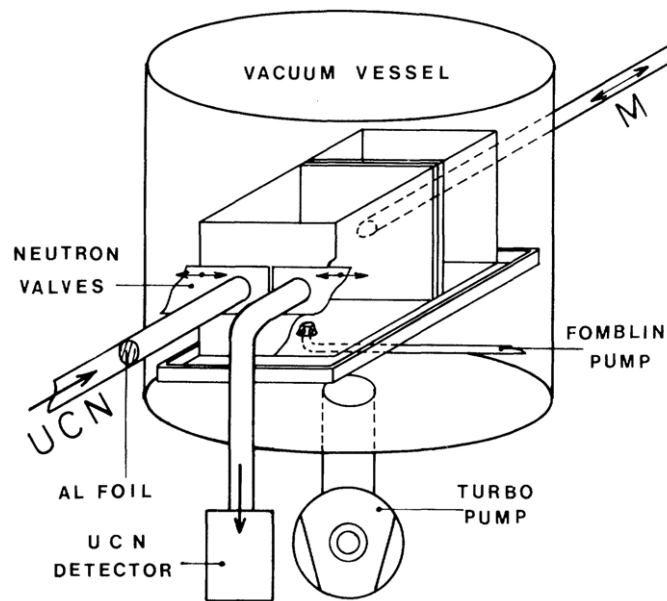


Figure 9. Schematic drawing of an experiment to measure the lifetime using UCN confined in a material bottle [82]. The volume of the confinement cavity can be changed allowing an extrapolation to zero surface-to-volume ratio, equivalent to a zero collision rate of neutrons with the cavity walls.

simultaneously measured the UCN storage time and the inelastically scattered neutrons [83], thus monitoring the primary loss process. Because neutrons can also occupy metastable orbits in the trap, it is necessary to ‘clean’ the energy spectrum by removing those UCNs so that the remaining losses are dominated by wall interactions.

A third approach exists to measure τ_n that, in principle, avoids the dominant systematic effects of both the beam and confinement techniques. The most natural way to measure exponential decay is to acquire an ensemble of radioactive species and register the decay products as a function of time. One can then simply fit the resulting time histogram for the slope of the exponential function. This method was first employed for neutrons in a magnetic storage ring. A magnetic gradient field imparts a force on a neutron $\mathbf{F} = -\nabla(\mu \cdot \mathbf{B})$. With the value of the neutron magnetic moment being about 60.3 neV T^{-1} , a neutron with energy of order 100 neV can be manipulated in the laboratory with tesla-size fields. The experiment was performed by storing very cold neutrons in a toroidal ring of magnetic sextupole fields and then counting the number remaining at various times after the initial fill. The number of events $N(t)$ was plotted as a function of time and fit with an exponential to extract the lifetime. The group obtained a value of $\tau_n = (877 \pm 10) \text{ s}$ [84].

Another experiment measures the lifetime using ultracold neutrons that are magnetically confined in superfluid ^4He [85]. The decay electrons are registered via scintillations in the helium thus allowing one to directly fit for the exponential decay of the trapped neutrons. The experiment has not yet produced a statistically competitive result, but efforts to reduce the uncertainty are in progress [86]. With advances in the density of stored ultracold neutrons and magnetic field technology, a number of groups propose to eliminate the losses from wall scattering in material bottles and trap the neutrons in a combination of magnetic field gradients and gravity [87].

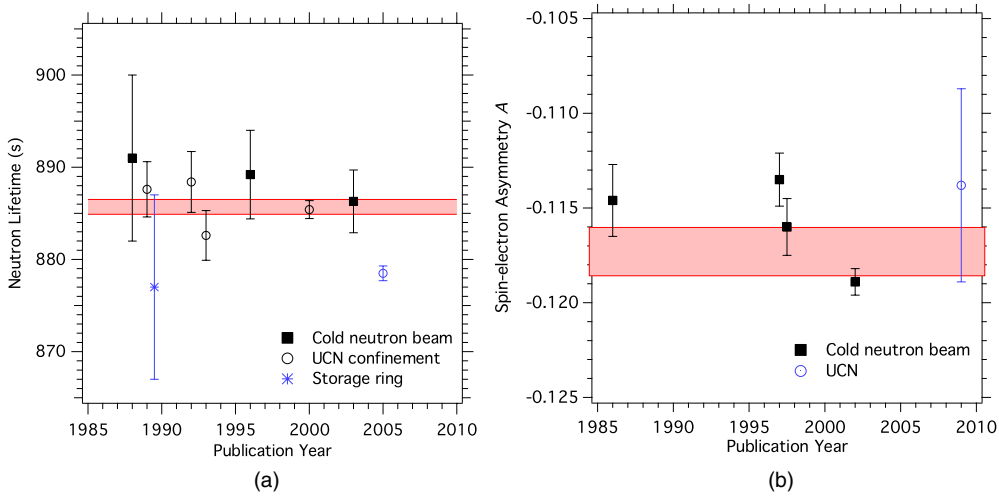


Figure 10. (a) A comparison of recent lifetime measurements. The shaded band represents the ± 1 standard deviation limits for the seven measurements (shown in black) included in the PDG evaluation. (b) The same comparison for recent measurements of A . The shaded band represents the limits for the four measurements (shown in black) included in the PDG evaluation; the limits are the uncertainty from the weighted average scaled by a factor of 2.3.

3.4. Status of neutron lifetime measurements

Accurate measurements using each of these distinct methods are important for establishing the reliability of the result for τ_n , particularly given a recent measurement that is significantly discrepant with the world average from the PDG 2008 evaluation. Figure 10(a) shows a summary of measurements over the last 20 years with competitive uncertainties. (A more historical and detailed review of neutron lifetime experiments is found elsewhere [88].) Seven of the experiments [81–83, 89–92] contribute to a current neutron lifetime world average of $\tau_n = (885.7 \pm 0.8)$ s [32]. The agreement among the measurements is very good. The experiments using beams do not have as much statistical influence as those using UCN, but they are also in good agreement.

Also shown in figure 10 is the most recent experiment that produced a value of $\tau_n = (878.5 \pm 0.8)$ s [93]. The result is more than six standard deviations away from the PDG average. The experiment used ultracold neutrons confined both gravitationally and by a material bottle and measured the total storage lifetime. The loss rate on the walls is given by $\tau_{\text{loss}}^{-1} = \eta\gamma$, where η is a wall-loss coefficient related to the probability of losing a neutron per interaction with the wall and γ is the loss-weighted collision frequency. Other loss mechanisms were considered negligible. The neutron lifetime was determined by extrapolating to zero collision frequency, as seen in figure 11. The experiment used low temperature fomblin oil to significantly reduce the value of η in comparison with previous experiments. The improvement reduced the size of the extrapolation necessary to extract τ_n , thus making the experiment less sensitive to some systematic effects. They also used two storage vessels with different surface-to-volume ratios and were able to change the energy distribution of the confined UCN, both of which change the collision frequency. The group intends to make additional measurements with a variable-volume trap to change the collision frequency while maintaining the same trap surface and vacuum conditions.

The substantial difference between the neutron lifetime of PDG average and that using the gravitational trap is not understood. It is essential to resolve the disagreement, and

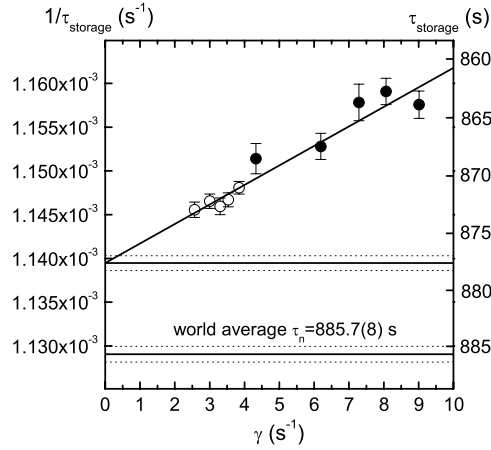


Figure 11. An extrapolation of the storage lifetimes to zero collision frequency. The plotting symbols correspond to two different trap geometries. Plot courtesy of A Serebrov.

it can only be accomplished through new measurements. Several experimental efforts are underway that include both refinement of existing experiments and techniques as well as development of new approaches [87]. Most of the proposed experiments use confined UCN because the systematic effects are thought to be less challenging. The beam experiments are very important because their set of systematic effects is distinct from those of the UCN confinement experiments. Agreement using the diverse techniques is needed for reliability of the value of the lifetime. The class of experiments that continuously monitor neutron decays must become more statistically competitive before they can make a significant statement, but the prospects are encouraging.

The question of how the value of $|V_{ud}|$ determined from the neutron beta-decay parameters τ_n and λ compares with those from the superallowed decays and CKM unitarity cannot be addressed without a resolution of the value of τ_n . New measurements of λ from neutron decay are also essential in establishing its reliability. In addition to experiments improving the precision of the spin-electron asymmetry [94], there are new efforts to improve the precision of the electron-antineutrino correlation that can provide independent measurements of λ that do not require polarimetry [95, 96].

4. Correlation coefficients

4.1. Spin-electron asymmetry A

The observable for A is the angular correlation between the neutron spin and the electron. More specifically, the probability that an electron is emitted with an angle θ with respect to the neutron spin is

$$W(E_e, \theta) \propto 1 + \beta P A \cos \theta, \quad (19)$$

where β is the ratio of the electron velocity to the speed of light and P is the neutron polarization. An experiment consists of measuring an asymmetry in electron counting rates as a function of the two neutron polarization states. Among the systematic concerns for an experiment, two of the more important ones are an accurate determination of the neutron polarization and the background subtraction, which must be known well for each neutron state.

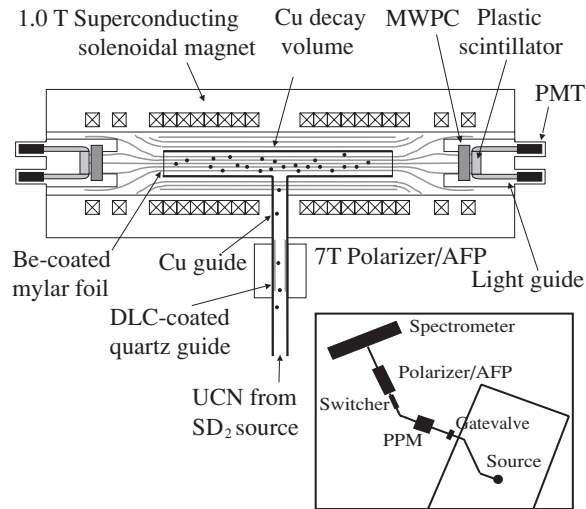


Figure 12. Schematic diagram of the UCNA apparatus. Figure courtesy of A Young.

With the neutron lifetime and one of the correlation coefficients, one can determine values for g_A and g_V . Because it has the greatest sensitivity to λ and is more accessible experimentally, A has been measured more frequently and with greater precision. As seen in figure 10(b) four independent measurements used in the PDG evaluation are not in good agreement with each other, and the PDG uses a weighted average for the central value and increases the overall uncertainty by a scale factor of 2.3 [32]. The two more recent measurements, one using an electron spectrometer and a new effort using ultracold neutrons, are also discussed.

The most precise determination of A comes from the group using the PERKEO II electron spectrometer. A beam of cold, polarized neutrons traversed a superconducting magnet in a split-pair configuration. The field was perpendicular to the beam direction, so neutrons passed through the spectrometer, but the decay electrons were guided by the field to one of two scintillator detectors on each end. This arrangement had the advantage of achieving a 4π acceptance of electrons. They form an asymmetry from the electron spectra in the two detectors as a function of the electron energy; the difference in those quantities for the two detectors is directly related to the electron asymmetry. Their run produced $A = -0.1178 \pm 0.0007$, where the main contributions to the uncertainty were attributed to the neutron polarimetry, background subtraction and electron detector response [94].

A subsequent run of the apparatus was performed to improve counting statistics and address some of the dominant systematic corrections and uncertainties. It used a ballistic supermirror guide [97] to increase significantly the counting rate and employed crossed supermirror polarizers to make the neutron polarization more uniform in phase space [98, 99]. The beam polarization was measured with a completely different method using an opaque ^3He spin filter [100]. A new result with smaller background and polarization corrections is anticipated.

A new effort to determine A using ultracold neutrons recently produced its first result. The UCNA Collaboration used a superconducting solenoidal spectrometer [101] to detect decay electrons from UCN, as shown in figure 12. The UCN are produced in a solid deuterium moderator and transported to the spectrometer where one produces highly polarized ($>99\%$) neutrons by passing them through a 6 T magnetic field and into an open-ended cylinder which

increased the dwell time of the polarized UCN in the decay spectrometer. The electrons were transported along the field lines to detectors at each end of the spectrometer. The detectors consisted of multiwire proportional counters backed by plastic scintillator. Extensive measurements of electron backscattering on electron detector materials were performed [102, 103]. The first result from an experiment to measure a decay correlation with UCN is $A = -0.1138 \pm 0.0051$ [104]. The uncertainty is not sufficiently small to shed any light on the disagreement among results for A , but it is statistics dominated. Data collection is ongoing, and it is reasonable to expect that a result with a total uncertainty that is competitive with existing experiments will be forthcoming.

One novel strategy to obtain λ without knowing the absolute neutron polarization is to measure both PA and PB simultaneously in the same apparatus (where P is the neutron polarization). This is possible by recognizing that $\lambda = (A - B)/(A + B)$. Thus, as long as the polarization is the same for measurements of both A and B , λ can be determined directly. This technique was employed in one experiment with the result $\lambda = -1.2686 \pm 0.0046$ [105], consistent with other determinations of λ obtained from measuring A alone.

4.2. Spin-antineutrino asymmetry B

The electron asymmetry and antineutrino asymmetry provide complementary information. Because g_A is nearly -1 in the SM, A is close to zero and B is near unity, B is not particularly sensitive to λ but is more sensitive to certain non-SM extensions, such as extended left–right symmetric models. This makes it a good system in which to search for SM extensions.

In particular, B may be considered in the context of the manifest left–right symmetric model (MLRM) where there are two intermediate vector bosons W_L and W_R that couple to left- and right-handed currents, respectively. The mass eigenstates W_1 and W_2 are given as superpositions of the weak eigenstates

$$W_1 = W_L \cos \zeta - W_R \sin \zeta, \quad (20)$$

$$W_2 = W_L \sin \zeta + W_R \cos \zeta, \quad (21)$$

where ζ is a mixing angle and $\delta = (M_1/M_2)^2$. A MLRM prediction for the functional dependence of B on δ and ζ gives

$$B = 2 \frac{\lambda^2(1 - y^2) - \lambda(1 - xy)}{(1 + x^2) + 3\lambda^2(1 + y^2)}, \quad (22)$$

where $x = \delta - \zeta$ and $y = \delta + \zeta$ [106]. If one assumes that $\zeta \approx 0$, then

$$B \approx B_{\text{SM}}(1 - 2\delta^2), \quad (23)$$

where B_{SM} is as given in table 2. Thus, with the measured value of B and B_{SM} (obtained with λ), one can determine a lower limit on the mass M_2 .

The observable for B is the angular correlation between the neutron spin and the antineutrino. Because the antineutrino cannot be conveniently detected, its momentum must be deduced from electron–proton coincidence measurements. In the last three decades, two groups have produced the most precise measurements of B . The approach of one group consisted of detecting electrons from the decay of polarized neutrons using plastic scintillators, and protons were detected by an assembly of two microchannel plates. From the electron energy and proton time of flight, they reconstructed the antineutrino momentum. Because B depends linearly on the neutron polarization, accurate polarimetry is essential and is consistently one of the main systematic concerns. The first measurement from this group produced a result of $B = 0.9894 \pm 0.0083$ [107]. A second run used largely the same

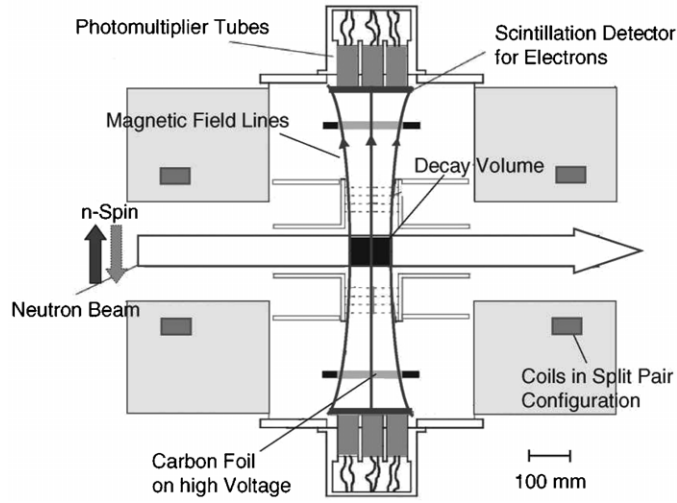


Figure 13. Schematic illustration of the PERKEO II apparatus [109]. The carbon foils serve to convert protons to electrons.

apparatus and measured $B = 0.9821 \pm 0.0040$ [108], where the largest reduction in the overall uncertainty came from improved statistics.

Two more recent measurements of B were performed using the PERKEO II apparatus [110]. Typically, one detects electron–proton coincidences using one detector for each particle. The PERKEO II measurement uses two detectors, one in each hemisphere of the detector, that can detect both electrons and protons. Electrons are detected using plastic scintillator, while the protons are accelerated on a thin carbon foil placed in front of the scintillator. The resulting secondary electrons are guided onto the electron detectors, as shown in figure 13. The corrections applied to these measurements were smaller than previous efforts. The beam polarization was achieved using crossed supermirror polarizers [99], an approach that gives a high degree of polarization with a smaller uncertainty. The more recent effort of this group yielded a result of $B = 0.9802 \pm 0.0050$, an uncertainty comparable with previous efforts [109].

Using the PDG value of B , largely determined by these measurements, and the value of B_{SM} with λ , one can establish a lower limit on the mass of M_{W_R} from equation (23) of $290 \text{ GeV}/c^2$ (90% CL) [109]. An analysis of muon decay experiments gives a limit on M_{W_R} of $549 \text{ GeV}/c^2$ and $|\zeta| \leq 0.0333$ [111]. The best direct search comes from $p\bar{p}$ collisions and sets a lower limit of $720 \text{ GeV}/c^2$ if one assumes that the right-handed neutrino is much lighter than W_R [112].

In the MLRM where there are only two parameters (ζ and δ), constraints from other systems are better than provided by neutrons and beta decays in general. For the extended left–right model, however, neutron-derived constraints are complementary to the other searches. In the framework of generalized left–right symmetric models, there are additional parameters that must be constrained: $r_g = g_R/g_L$, the ratio of the two gauge coupling strengths g_L and g_R , and $r_K = V_{ud}^R/V_{ud}^L$, where $V_{ud}^{R,L}$ are the matrix elements of the CKM matrices pertaining to the R/L-sectors. In the MLRM, $r_g = r_K = 1$. Here information from beta decay is complementary to these results and therefore highly desirable. In addition, a recent analysis has investigated the sensitivity of B to the minimal supersymmetric standard model [113].

New measurements would have to investigate the energy dependence of B below 10^{-3} , a level that may be feasible for a new generation of experiments.

Another area in which to search for right-handed currents is the decay of the neutron into a hydrogen atom and antineutrino because one of the hyperfine levels of hydrogen in this decay mode cannot be populated unless right-handed currents are present (see section 5.2). The very small branching ratio to this decay channel has undoubtedly served to deter searches thus far.

4.3. Spin-proton asymmetry C

The main efforts in determining λ have centered around precision measurements of the spin-electron asymmetry A . Independent checks on λ , however, are essential for confidence in testing $V-A$ theory in the neutron system, and it naturally leads one to look at other approaches. The proton asymmetry C is an obvious choice because of its acceptable sensitivity to λ , but in addition, a precision measurement of C has sensitivity to recoil-order effects, such as the hadronic current, weak magnetism form factor and the Fierz interference term [114–116]. The first-order radiative and recoil corrections have been calculated as well as an analysis of the sensitivity of C to models beyond the SM [117].

Physically, the proton asymmetry describes the angular distribution of the proton relative to the polarized neutron. Kinematically, it is coupled to the other decay products and therefore must be proportional to both the electron and antineutrino asymmetries

$$C = x_C(A + B), \quad (24)$$

where the proportionality constant $x_C = 0.27484$ is a kinematic factor [115, 118]. As its name suggests, the asymmetry may be formed experimentally by counting the number of protons in one hemisphere versus the other where the orientation is defined by the neutron spin [119]. The only measurement of C was performed with the PERKEO II spectrometer. The apparatus was essentially the same as that used to measure B (see figure 13). A value of $C = -0.2377 \pm 0.0026$ was obtained, and the uncertainty was dominated by detector calibration issues [120]. In order to contribute significantly to the determination of λ or begin to constrain some of the non-SM models, however, the experimental precision must be improved by about an order of magnitude.

4.4. Electron–antineutrino correlation a

Even though the electron–antineutrino correlation a has approximately the same sensitivity as A (see table 2), the precision of existing experiments is only about 4%. One contributing factor is that measurements of a have typically involved precise measurement of the proton energy spectrum. This type of measurement is intrinsically difficult to do because a manifests itself as a small deviation in the shape of a spectrum whose endpoint is only 751 eV. Regardless, the most probable arena for a measurement of λ approaching the same level of precision as that in A comes from new efforts to determine a [121].

Because the correlation coefficients overconstrain the $V-A$ description of neutron decay, one can test the self-consistency and validity of the model description without any model-dependent ambiguities [122]. Based on the expressions from table 2, one can construct two equations

$$F_1 \equiv 1 + A - B - a = 0 \quad \text{and} \quad (25)$$

$$F_2 \equiv aB - A - A^2 = 0. \quad (26)$$

Using the PDG 2008, compilation for the coefficients yields $F_1 = 0.0050 \pm 0.0052$ and $F_2 = 0.0025 \pm 0.0041$, where the uncertainty in a limits the precision of the comparison [96].

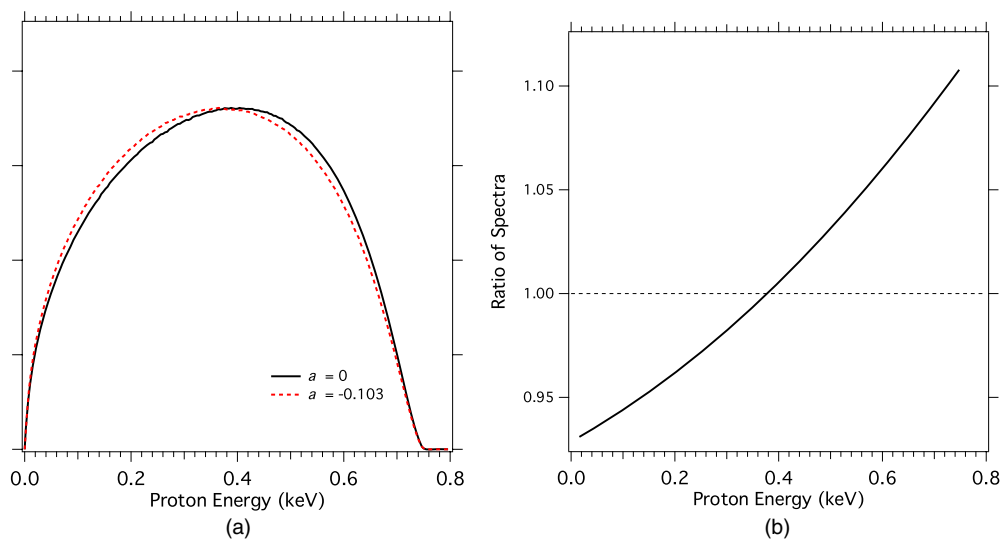


Figure 14. (a) The deviation in the proton kinetic-energy spectrum due to the influence of a . (b) The ratio of the two spectra indicating the size of the effect one measures for a .

The values are in good agreement with the $V - A$ theory, but even a small improvement in a would make this comparison much more useful. In addition to contributing to an improved test of CKM unitarity, a precise comparison of a and A can place stringent limits on possible conserved-vector-current violation and second class currents in neutron decay [123].

An advantage in measuring a is that it does not involve the neutron spin and hence precision polarimetry is not required. Since an experiment in 1978 [124], however, there has been only one measurement. Its experimental difficulty lies with the energy measurement of the recoil protons, whose spectral shape is slightly distorted for a nonzero a . Physically, a describes that the angular distribution between the electron and the antineutrino, and kinematically, it must therefore affect the average momentum imparted to the recoiling proton. The strength of this correlation produces an alteration in the kinetic energy spectrum of the proton; figure 14 illustrates the difficulty in isolating the distortion.

The most recent determination of a comes from measurements of the integrated energy spectrum of recoil protons stored in an ion trap [125]. A collimated beam of cold neutrons passed through a proton trap consisting of annular electrodes coaxial with a magnetic field whose strength varied from 0.6 T to 4.3 T over the length of the trap. Protons created inside the volume were trapped, and those created in a high field region were adiabatically focused onto a mirror in the low field region. The trap was periodically emptied and the protons counted as a function of the mirror potential. The result of $a = -0.1054 \pm 0.0055$ is in good agreement with the previous measurement and of comparable precision.

Two experiment efforts are underway that plan to push the relative uncertainty to the 0.5% level or better. In the a SPECT experiment [126], one again measures a proton energy spectrum as a function of a potential, similar to the idea used for the proton trap experiment. One increases the statistical power by completely separating the source part and the spectroscopy part of the apparatus. A cold neutron beam passes through a region of strong, homogeneous magnetic field transverse to the beam. The decay protons with an initial momentum component along the field direction are directed toward a detector. Near the detector is a region of

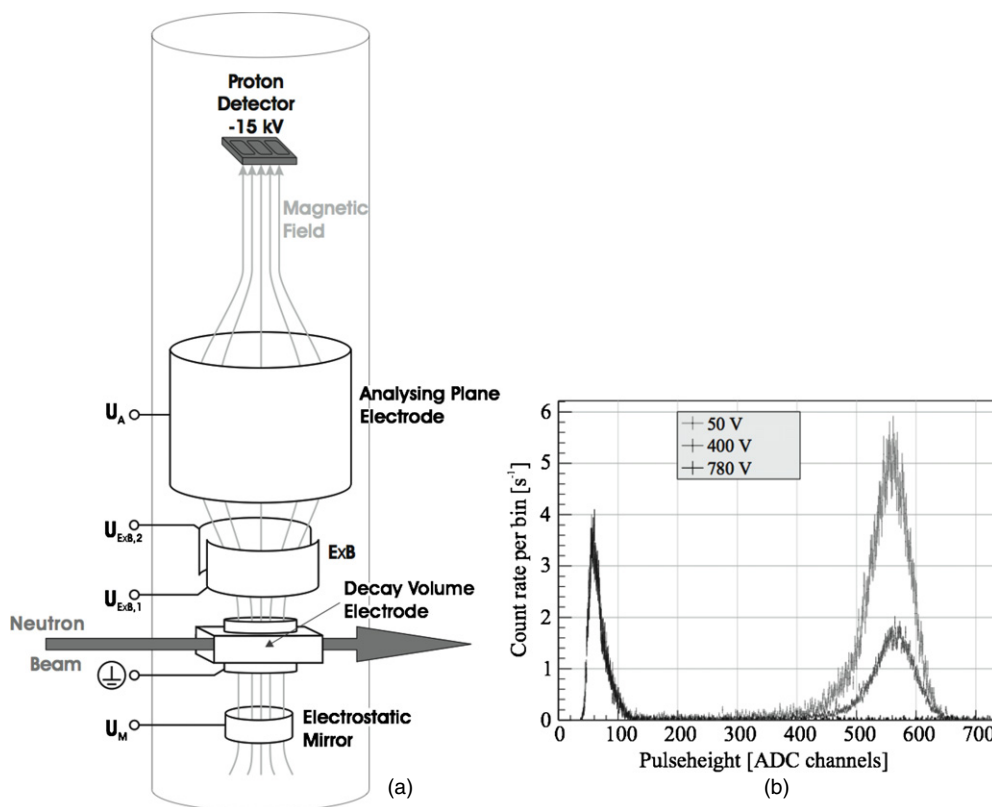


Figure 15. (a) Schematic illustration of the detection principle for the *a*SPECT spectrometer. (b) Plot showing the proton pulseheight for three voltages of the analyzing plane. It demonstrates the ability of the spectrometer to analyze the proton energies necessary for extracting *a*. Plots courtesy of S Baeßler.

the weaker magnetic field and electrostatic retardation potentials, and only those protons with sufficient energy to overcome the barrier continue on to the detector [95], as shown in figure 15. Registering the protons as a function of the retardation potential gives the recoil proton spectrum, which one fits to extract *a*. The collaboration believes that a statistical uncertainty of approximately 0.3% is achievable and has completed initial measurements with the apparatus [127].

The approach of the aCORN collaboration will employ a novel technique that forms an asymmetry in the coincidence detection of electrons and recoil proton that is proportional to *a* [128]. The asymmetry is formed by carefully restricting the phase space for the decay in a magnetic spectrometer so that decay events with parallel and antiparallel electron and antineutrino momenta are separated in the coincidence timing spectrum. In general, there will be two groups of protons whose momentum depends on the initial direction of the antineutrino, and one group will be slower than the other. By limiting the maximum transverse momentum of the proton, one can ensure that the solid angle for these two groups are identical, in which case an observed asymmetry results directly from a non-zero value of *a* [96]. The measured time of flight between the electron and proton is used to assign each decay event to its proper group, as illustrated in figure 16. This approach has the advantage of determining *a* as a count

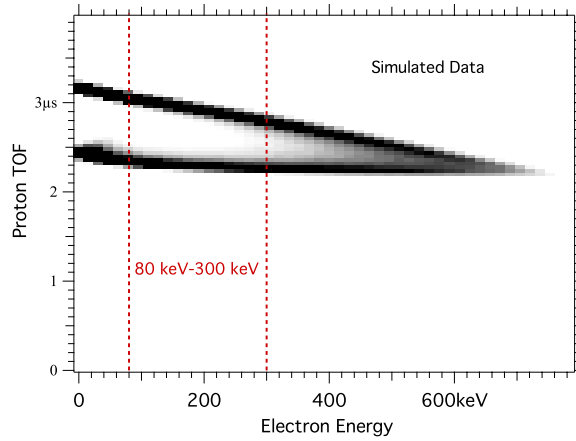


Figure 16. Simulation of the proton time of flight versus the electron energy for the aCORN experiment. The two groups of protons are well separated for electron energies below 300 keV. Plot courtesy of F Wietfeldt.

asymmetry, thus there is no need for precise spectroscopy of the low energy protons, but the cost is a significant reduction in count rate, a consequence of restricting the phase space.

The Nab Collaboration develops an electromagnetic spectrometer that would guide both decay electrons and protons to detectors at each end of the spectrometer [129]. The goal is to measure a and the Fierz interference term b in the same apparatus. The detectors would be large-area segmented silicon detectors with thin entrance windows that allow the detection of both the proton and electron. The ability to detect coincidences greatly suppresses backgrounds and allows the measurement of residual backgrounds. The magnetic field guides the decay products to conjugate points on the segmented Si detectors and provides 4π detection of both electrons and protons and suppression of backgrounds by use of coincidences [130].

The electron–antineutrino asymmetry provides one of best avenues for an independent determination of λ . The prospect for a significantly improved limit within the next several years is very good.

4.5. Fierz interference b

In the $V - A$ formalism of neutron decay, there are no interactions that would give rise to a deviation in the electron spectrum analogous to a . This makes a precision measurement of the electron energy spectrum a natural place to look for non- $V - A$ interactions. There are both Fermi and Gamow–Teller contributions to the Fierz term (i.e., $b = b_F + b_{GT}$) that can be expressed as

$$b_F = \frac{C_S C_V}{|C_S|^2 + |C_V|^2} \quad \text{and} \quad b_{GT} = \frac{C_T C_A}{|C_T|^2 + |C_A|^2}. \quad (27)$$

These terms vanish for purely right-hand coupling and are non-zero for left-hand coupling if there exist scalar or tensor interactions. A recent analysis has investigated the sensitivity of the Fierz term to supersymmetric models, and it is interesting to note that small improvements in the present limit on b will start to have an impact on the maximum allowed range [113].

To date, there are no measurements of b that come from experiments using neutrons. The limit on b comes only from nuclear decays. To extract a limit, one plots the $\mathcal{F}t$ -values of

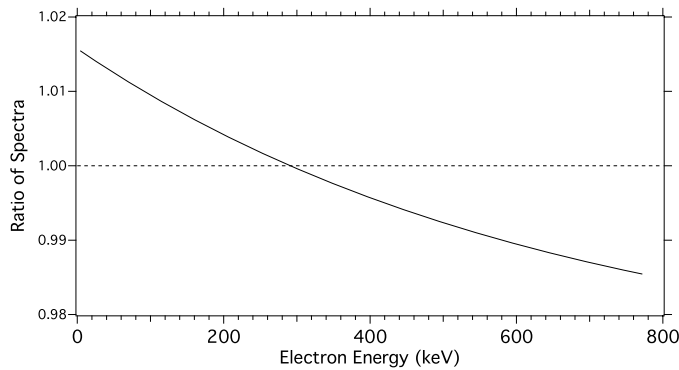


Figure 17. The plot shows the ratio of the electron spectrum for $b = 0.05$ to one with $b = 0$ (i.e., figure 3(b)). For a large value of b already disallowed by experiment, note the small influence of b on the energy spectrum in comparison with that of a in figure 14.

superallowed $0^+ \rightarrow 0^+$ decays as a function of Z of the nucleus. The values may be fit to a function allowing the possibility of a non-zero b . An analysis of the $\mathcal{F}t$ -values yields a limit of $b_F = +0.0001 \pm 0.0026$ [60]. Measurement of the shape of the positron energy spectrum in the decay of ^{22}Na gives the best limit of $b_F = +0.0008 \pm 0.0028$ [131].

Experimentally, a non- $V - A$ interaction in neutron decay would produce an alteration in the spectrum that is inversely proportional to the electron energy, as seen in equation (11). Thus, an experiment intent on limiting b in the neutron should be able to perform accurate low-energy electron spectroscopy. Figure 17 shows how a value of $b = 0.05$ would perturb the spectrum. Note that this fairly large value of b produces a maximum deviation at zero energy of only 1.5%, and any potential experiment must contend with energy-dependent systematics that could alter the spectrum in a similar manner. Electron backscattering is one such example. Backscattering from silicon or plastic, two common materials for electron detection, is very large ($\approx 10\%$) at the relevant energies of around 100 keV. The only experimental effort directed toward measuring b comes from the Nab Collaboration, but a measurement producing an uncertainty that is competitive with existing limits is probably several years away.

Regardless, the sensitivity of b to new physics should give impetus for addressing the experimental challenges. One should note that the current limit produced by the nuclear decays comes from a large number of experiments collected over several decades. As such, it is unlikely that any one additional experiment will significantly improve that limit, but should a radioactive beam facility with a higher intensity than existing sources come online, such as FRIB [132], those prospects could change. Regardless, experiments that search for a Fierz term would be a fruitful area for future neutron research.

4.6. Triple correlation D

The T -violating term from equation (11) is expressed in terms of the neutron spin, electron momentum and antineutrino momentum as $\langle \mathbf{J} \rangle \cdot (\mathbf{p}_e \times \mathbf{p}_\nu)$. Using momentum conservation, one can rewrite the triple correlation in terms of the observable \mathbf{p}_p . A non-vanishing difference between the measurements of the triple-correlation coefficient for the two neutron spin states implies a violation of motion reversal.

In the last decade, there have been two experimental efforts, EMiT and Trine, to improve the limit on the D coefficient in neutron decay. Each requires an intense, longitudinally polarized

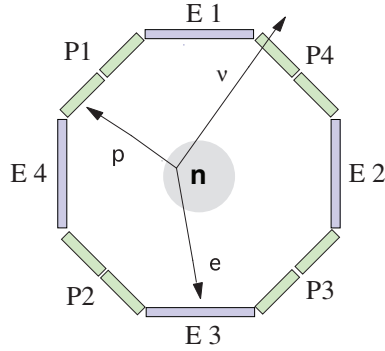


Figure 18. Schematic illustration of an experiment to measure the D -coefficient. Alternating electron and proton detectors surround a beam, and data are collected in electron–proton coincidence pairs as a function of the neutron spin state. A D coefficient would manifest itself as a non-zero difference in rates of coincidence events in those two states.

beam of cold neutrons around which one places proton and electron detectors alternating in azimuth, as shown in figure 18. Coincidence data are collected in electron–proton pairs as a function of the neutron spin state to search for the triple correlation.

In the EMiT experiment, the detector consisted of four electron detectors and four proton detectors arranged octagonally around the neutron beam [133]. The octagonal geometry maximized the experiment’s sensitivity to D by balancing the sine dependence of the cross product with the large angles between the proton and electron momenta that are favored by kinematics. The decay protons drifted in a field free region before being focused by a -30 kV to -37 kV potential into an array of PIN diode detectors. With its maximum recoil energy of 751 eV, most of the protons arrived approximately $1 \mu\text{s}$ after the electrons. Detector pairs were grouped in the analysis to reduce potential systematic effects from neutron transverse polarization. The result from the first run of EMiT yielded a limit of $D = [-0.6 \pm 12(\text{stat}) \pm 5(\text{sys})] \times 10^{-4}$ [133].

The best constraint on D comes from the Trine Collaboration, which reports $D = [-2.8 \pm 6.4(\text{stat}) \pm 3.0(\text{sys})] \times 10^{-4}$ [134]. They used two proton detectors and two electron detectors in a rectangular geometry. The proton detectors were comprised of arrays of thin-window, low-noise PIN diodes. The detectors were held at ground while the neutron beam was surrounded by a potential of -25 kV; the field was shaped to focus the decay protons onto the PIN arrays. The electrons were detected by plastic scintillators in coincidence with multi-wire proportional chambers. This coincidence provided reduction in the gamma-ray background rates and positional information on the decay, thus minimizing some sources of systematic uncertainty.

The PDG evaluation obtains a new value for the neutron D coefficient of $(-4 \pm 6) \times 10^{-4}$, which constrains the phase of g_A/g_V to $180.06^\circ \pm 0.07^\circ$ [32] and is comparable to the limit obtained in the beta decay of ^{19}Ne , where $D_{^{19}\text{Ne}} = (1 \pm 6) \times 10^{-4}$ [135]. Neither of the neutron experiments was limited by systematic effects, and thus both would benefit by more running time and higher flux. Both collaborations upgraded their detectors and performed second runs [136, 137]. Figure 19 shows the history of D experiments. In the near future, it is reasonable to anticipate new results that will put a limit on D very near 10^{-4} . With the recent calculation of the D final-state interactions [73], an experimental limit near that level is

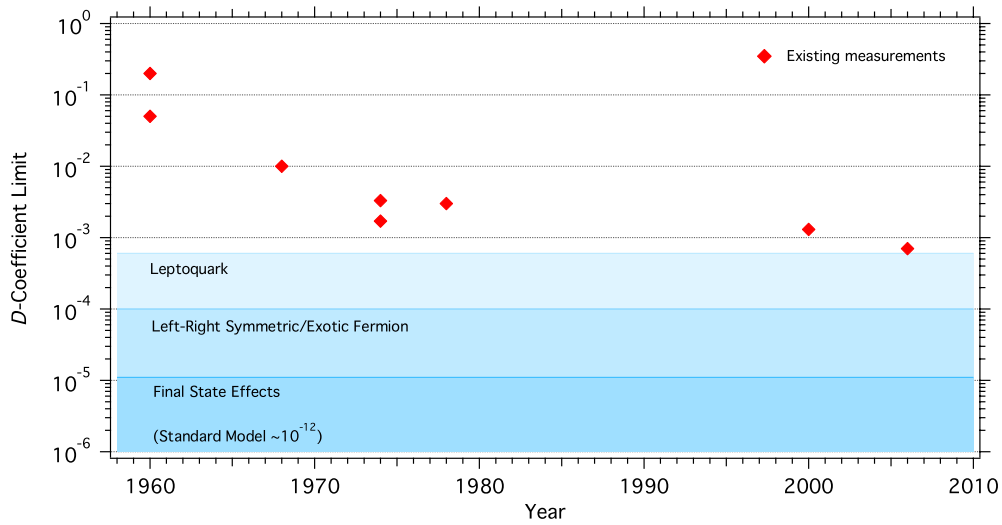


Figure 19. The progress of D -coefficient measurements over time. The points give the upper limit from particular experiments. The shaded regions give the current upper limits by some theories that are potentially accessible by new experiments.

desirable not only to test the calculations of weak magnetism directly but to use it to limit the extent of theory predictions.

4.7. R and N correlations

While most of the experimental studies of \mathcal{T} -invariance in the neutron have centered around the D coefficient, another \mathcal{T} -odd correlation present in neutron decay is the R correlation, $R\sigma \cdot (\langle \mathbf{J} \rangle \times \mathbf{p}_e)$. Physically, the R coefficient represents a transverse component of the electron polarization relative to the plane perpendicular to the neutron spin.

Although the best limits on R come from the nuclear decays, a recent experiment made the first measurement of R from the neutron. It used a Mott electron polarimeter placed on two opposite halves of a polarized cold-neutron beam, as illustrated in figure 20. The polarimeter consisted of a multi-wire proportional counter, a lead foil and a plastic scintillator detector. The proportional counter provided particle identification that is important for background rejection, and the scintillator measured the electron energy. The analyzing foil could be taken in and out of the polarimeter to obtain the peak of the Mott scattering distribution. To extract the coefficient, an asymmetry was formed by flipping the spin of the neutron. The result for R from this measurement is 0.008 ± 0.016 [50]. The value is consistent with \mathcal{T} invariance and improves existing limits on scalar couplings.

The polarimeter was capable of measuring both transverse components of the electron polarization, i.e., the component perpendicular to the decay plane determined by the neutron spin and electron momentum and the component within the same decay plane. As such, the apparatus was able to measure another decay correlation requiring electron polarimetry without requiring significant experimental modifications. In contrast to R , the N correlation is \mathcal{T} even and is nonzero in $V - A$ theory; its expression is given by $N(\sigma \cdot \langle \mathbf{J} \rangle)$. Its first measurement yielded $N = 0.056 \pm 0.012$, a value consistent with the SM [50]. Although it

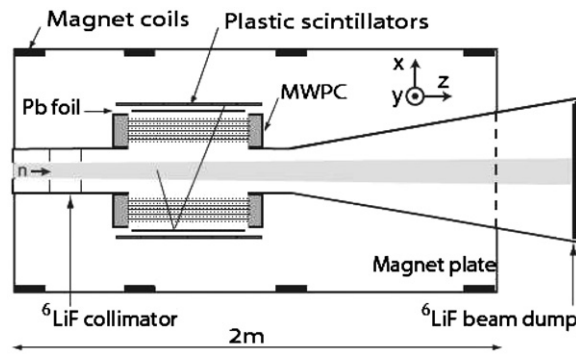


Figure 20. Schematic illustration of an experiment to measure the R correlation [50]. The cold neutron beam passes through the center of the polarimeter; an example of a decay electron track is shown by the solid line.

does not contribute significantly to the determination of λ , it does serve to help demonstrate the validity of the operation of the apparatus.

5. Other decay modes

5.1. Radiative neutron decay

Although neutron decay is typically considered as a three-body process, in the radiative correction it is always accompanied inner-bremsstrahlung (IB) photons, $n \rightarrow e^- + p + \nu_e + \gamma$. While IB has been measured in nuclear beta decay and electron capture decays, it has only recently been observed in free neutron beta decay.

The photon energy spectrum and branching ratio were calculated within a quantum electrodynamics (QED) framework [138]. Those same parameters as well as the photon polarization were also calculated using heavy baryon chiral perturbation theory (HB χ PT) including explicit Δ degrees of freedom [47, 48]. The QED calculation takes into account electron IB while the HB χ PT calculation includes all terms to order $1/M$ (where M is the nucleon mass) including photon emission from the effective weak vertex. These additional terms contribute at the level of less than 0.5% and create only a slight change in the photon spectrum and branching ratio. Both the photon energy spectrum and the photon polarization observables are dominated by electron IB.

The experimental challenge was to distinguish the very low rate of radiative decay events in the large photon background of a neutron beam. Given the long neutron lifetime and the branching ratio above 15 keV being only about 3×10^{-3} , the rate of detectable photons is quite small. The first experiment to search for this decay mode resulted in an upper limit of 6.9×10^{-3} (at the 90% confidence level) for the branching ratio of photons between 35 keV and 100 keV [139]. A more recent effort was able to definitively detect the radiative photons and measure the branching ratio at the 10% level [140]. In both experiments, the signature of the radiative decay event is the detection of the decay electron and radiative photon in prompt coincidence. The very low rate of these events is insufficient to make it measurable above the large rate of random coincidences. In the both experiments, the solution uses detection of the delayed proton (due to its lower kinetic energy) as a powerful suppression of background events.

For the case of the experiment in [140], this additional suppression along with significant gamma shielding and a large solid angle for charged particle detection was sufficient to measure definitively the branching ratio. The apparatus allowed the detection of a photon and an electron in coincidence followed by a delayed proton using a strong (4.6 T) magnetic field [141]. It constrained the proton and electron to cyclotron orbits, which increased the solid angle for detection and minimized uncorrelated backgrounds. An electrostatic mirror was used to vary the rate of detected electron–proton coincidences without changing the uncorrelated photon background rate, thus providing a signature for the detection of radiative decay and an important systematic check on possible backgrounds. Photons with energies between 15 keV and 340 keV were detected by a scintillating crystal coupled to an avalanche photodiode and were distinguished from uncorrelated background photons by coincidence with both the decay electron and proton [142]. Correlated background from external bremsstrahlung generated in the electron detector was estimated to contribute less than 3% of the radiative decay event rate. The branching ratio was measured to be $(3.13 \pm 0.34) \times 10^{-3}$ and is consistent with the theoretical predictions of 2.85×10^{-3} in the same energy region.

Only a small fraction of the solid angle for photon detection was utilized in that experiment. A new experiment is in progress that should permit a precision measurement of the photon energy spectrum and the branching ratio at approximately the 1% level. Its most significant improvement is utilizing a photon detector that has about an order of magnitude more solid angle coverage. An improved measurement of the photon spectrum below the 1% level could examine effects beyond the leading order electron bremsstrahlung. A measurement of the photon circular polarization could reveal information about the Dirac structure of the weak current [47, 138]. Furthermore, access to the radiative photon opens the possibility of new areas of investigation for neutron beta decay [143]. For example, the principle of the measurement could be reversed and the radiative photon could be used as a tag for definitively identifying neutron decay products, or the use of a polarized neutron beam may allow the investigation of new angular correlations with photon and neutron polarization.

5.2. Neutron decay into hydrogen

Another decay process available to the neutron is the two-body decay into a neutral hydrogen atom and an antineutrino, $n \rightarrow \text{H}^0 + \bar{\nu}_e$ [144]. It has been understood for many years that the decay into hydrogen would provide a sensitive probe for studying the weak interaction, in particular the existence of right-handed currents [145] or scalar and tensor couplings. The back-to-back decay produces two particles of fixed energy, $E_{\bar{\nu}} = 782$ keV and $E_H = 326$ keV. Only the S-states of the hydrogen atom will be populated because only these states have a non-zero overlap of the proton and electron wavefunctions. The branching ratio for this mode into one of these hyperfine structure states is highly suppressed but has been calculated in the standard $V - A$ theory to be approximately 4×10^{-6} [144–146]. This very small branching ratio has deterred any experimental investigations thus far although an indirect estimation can be made by comparing the value of the neutron lifetime obtained from disappearance-type versus appearance-type experiments [147].

Non- $V - A$ physics can be addressed by measuring the populations of the hyperfine states. The pure, left-handed $V - A$ interaction predicts with sufficient precision the populations based on the spin projections of the initial particles [148]. Admixtures of scalar or tensor couplings will change those relative populations, thus providing evidence for new interactions. Regarding right-hand currents, one of the hyperfine levels is forbidden by the conservation of total angular momentum. Thus, detection of a non-zero population in that state would provide an unambiguous signature for right-handed currents.

This strong physics motivation has produced an ambitious experimental effort to detect the decay mode and measure the relative hyperfine populations [149]. The approach would use a tangential through-port on a reactor neutron source, where the neutron flux is very high. The hydrogen atoms drift from the core through a Lamb-shift polarimeter to select the desired hyperfine state. The atoms are then resonantly ionized and the resulting proton is detected. It is important to measure the energy of the proton because it serves as a strong method of rejecting background protons, as the number of background hydrogen atoms with the same kinetic energy as those from neutron decay should be small.

6. Summary

There has been much progress in the study of neutron beta-decay physics in recent years and the activity is only increasing. The status of the comparison of parameters from neutron decay with the SM and the results from superallowed nuclear decays is very good. The accomplishments of the nuclear systems, specifically the determination of V_{ud} , have been a remarkable success in testing the SM and also limiting its possible extensions. Naturally, there remain outstanding questions that must be addressed to remove lingering questions and continue to improve the comparison. Much of the work extends beyond the nuclear beta-decay system. In particular, the uncertainty in V_{us} contributes a significant amount to the test of CKM unitarity and needs to be reduced both experimentally and theoretically.

It is quite feasible to reach, or even surpass, a comparable precision in the neutron-decay system, but unresolved experimental problems are presently precluding improvement. It is not the statistical precision of experiments but rather the spread in the central values among experiments that is the core issue. Some experiments have underestimated systematic effects, and it is clear that new experiments are necessary to resolve discrepancies.

Knowledge of the neutron lifetime, where measurements had shown good consistency for more than two decades, is again uncertain with the most precise measurement being more than six sigma from the PDG 2008 average. The situation is presently unacceptable but significant efforts are directed toward a resolution. New techniques using magnetically confined UCN that reduce concerns about wall interactions are being developed, and improvements of existing techniques using both UCN and cold neutrons are ongoing. It is reasonable to think that the disagreement in the lifetime will be resolved in the near future, and also that its uncertainty will be reduced significantly below the 1 s level.

The largest factor contributing to the uncertainty in the determination of V_{ud} in the neutron comes from λ , but it is important to note that it predominantly arises from the application of a scale factor to cover the dispersion in the measurements of the spin-electron asymmetry. The uncertainty in individual measurements is significantly less and is expected to be much smaller from measurements already in progress. The most precise experiment has greatly improved the dominant corrections and systematic effects and continues to do so, but it is still unsatisfying not to have confirmation from another experiment at a similar level of precision. Fortunately, the prospects for doing so are quite good; they come from an experiment to measure A using ultracold neutrons and also from efforts to significantly improve the somewhat neglected electron–antineutrino correlation a .

Studies of \mathcal{T} invariance with neutron correlations should continue to improve. Neither of the recent D -coefficient experiments were limited by systematic effects, and it is feasible that new efforts could approach the level of final-state interactions. The first measurement of the R coefficient already makes a significant improvement in the limits on the relative strength of imaginary scalar couplings.

There are a number of new ideas in neutron beta decay that may come to fruition in the coming years. The possibility of measuring correlations, not just the lifetime, with high statistics using ultracold neutrons is an intriguing prospect that could provide competitive uncertainties but with dramatically different systematic effects. The detection of neutron decay directly into hydrogen affords the exciting possibility of supplying an unambiguous signature for right-handed currents. There is also proposal to build a high-flux source of neutron decay products that could greatly enhance the statistical power for angular correlation measurements [150]. Although still a relatively small field compared to other areas in nuclear and particle physics, the opportunities in neutron beta-decay physics are growing and should yield even more results.

Acknowledgments

The author would like to S Baeßler, K Bodek, K J Coakley, R L Cooper, M S Dewey, C Fu, S Gardner, T Gentile, J McGovern, A Serebrov, T Soldner, F E Wietfeldt and A Young for their contributions to this paper including informative discussions, providing figures or a careful reading of the paper. The author acknowledges the support of the NIST Physics Laboratory and Center for Neutron Research.

References

- [1] Glashow S 1961 *Nucl. Phys.* **22** 579
- [2] Weinberg S 1967 *Phys. Rev. Lett.* **19** 1264
- [3] Salam A 1968 *Proc. 8th Nobel Symp.* 367
- [4] Lee T D and Yang C N 1956 *Phys. Rev.* **104** 254
- [5] Wu C S, Ambler E, Hayward R W, Hoppes D D and Hudson R P 1957 *Phys. Rev.* **105** 1413
- [6] Garwin R L, Lederman L M and Weinrich M 1957 *Phys. Rev.* **105** 1415
- [7] Schramm D N and Wagoner R V 1977 *Annu. Rev. Nucl. Part. Sci.* **27** 37
- [8] Lopez R E and Turner M S 1999 *Phys. Rev. D* **59** 103502
- [9] Burles S, Nollett K M, Truran J W and Turner M S 1999 *Phys. Rev. Lett.* **82** 4176
- [10] Byrne J 1982 *Rep. Prog. Phys.* **45** 115
- [11] Byrne J 1995 *Phys. Scr. T* **59** 311
- [12] Dubbers D 1999 *Nucl. Phys. A* **654** 297c
- [13] Nico J S and Snow W M 2005 *Annu. Rev. Nucl. Part. Sci.* **55** 60
- [14] Severijns N, Beck M and Naviliat-Cuncic O 2006 *Rev. Mod. Phys.* **78** 991
- [15] Abele H 2008 *Prog. Part. Nucl. Phys.* **60** 1
- [16] Turchin V F 1965 *Slow Neutrons* (Jerusalem: Israel Program for Scientific Translations)
- [17] Krupchitsky P 1965 *Fundamental Research with Polarized Slow Neutrons* (Berlin: Springer)
- [18] Alexandrov Y A 1992 *Fundamental Properties of the Neutron* (Oxford: Clarendon)
- [19] Bryne J 1994 *Neutrons, Nuclei, and Matter* (Bristol: Institute of Physics Publishing)
- [20] Commins E D and Bucksbaum P H 1983 *Weak Interactions of Leptons and Quarks* (Cambridge: Cambridge University Press)
- [21] Holstein B R 1989 *Weak Interactions in Nuclei* (Princeton, NJ: Princeton University Press)
- [22] Grotz K and Klapdor H V 1990 *The Weak Interaction in Nuclear, Particle and Astrophysics* (Bristol: Institute of Physics Publishing)
- [23] Zimmer O, Butterworth J, Nesvizhevsky V and Korobkina E 2000 *Nucl. Instrum. Methods A* **440** 471–815
- [24] Ball P, Flynn J, Kluit P and Stocchi A 2003 *Proc. 2nd Workshop on the CKM Unitarity Triangle* (Durham, NC: IPPP) arXiv:[hep-ph/0304132](https://arxiv.org/abs/hep-ph/0304132)
- [25] Arif M, Dewey M S, Gentile T R, Huffman P R and Nico J S 2005 *J. Res. Natl. Inst. Stand. Technol.* **110** 137–496
- [26] *Proc. Int. Workshop on Particle Physics with Slow Neutrons, 29–31 May 2008, Grenoble, France* unpublished
- [27] Erler J and Ramsey-Musolf M J 2004 *Prog. Part. Nucl. Phys.* **54** 351
- [28] Chadwick F 1932 *Proc. R. Soc. Lond. A* **136** 692
- [29] Chadwick F and Goldhaber 1934 *Nature* **134** 237

- [30] Snell A and Miller L 1948 *Phys. Rev.* **74** 1217A
- [31] Fermi E 1949 *Nuclear Physics* (Chicago, IL: University of Chicago Press)
- [32] Amsler C *et al* 2008 *Phys. Lett. B* **667** 1 (Particle Data Group)
- [33] Sears V F 1989 *Neutron Optics* (Oxford: Oxford University Press)
- [34] Luschikov V I, Pokotolovsky Y N, Strelkov A V and Shapiro F L 1969 *Sov. Phys. JETP Lett.* **9** 23
- [35] Steyerl A 1969 *Phys. Lett. B* **29** 33
- [36] Golub R and Pendlebury J M 1977 *Phys. Lett. A* **62** 337
- [37] Ageron P, Mampe W, Golub R and Pendlebury J M 1978 *Phys. Lett. A* **66** 469
- [38] Saunders A *et al* 2004 *Phys. Lett. B* **593** 55
- [39] Liu C Y and Young A R 2004 arXiv:nucl-th/0406004
- [40] Czarnecki A, Marciano W J and Sirlin A 2005 *Phys. Rev. D* **70** 093006
- [41] Towner I S and Hardy J C 1995 *Symmetries and Fundamental Interactions in Nuclei* ed W C Haxton and E M Henley (Singapore: World Scientific)
- [42] Towner I S and Hardy J C 2003 *J. Phys. G: Nucl. Part. Phys.* **29** 197
- [43] Marciano W J and Sirlin A 2006 *Phys. Rev. Lett.* **96** 032002
- [44] Jackson J D, Treiman S B and Wyld H W 1957 *Phys. Rev.* **106** 517
- [45] Ando S, Fearing H W, Gudkov V, Kubodera K, Myhrer F, Nakamura S and Sato T 2004 *Phys. Lett. B* **595** 250
- [46] Torres J J, Flores-Mendieta R, Neri M, Martínez A and García A 2004 *Phys. Rev. D* **70** 093012
- [47] Bernard V, Gardner S, Meißner U G and Zhang C 2004 *Phys. Lett. B* **593** 105
- [48] Bernard V, Gardner S, Meißner U G and Zhang C 2004 *Phys. Lett. B* **599** 348
- [49] Gudkov V, Kubodera K and Myhrer F 2005 *J. Res. Natl. Inst. Stand. Technol.* **110** 315
- [50] Kozela A *et al* 2009 *Phys. Rev. Lett.* **102** 172301
- [51] Cabibbo N 1963 *Phys. Rev. Lett.* **10** 531
- [52] Kobayashi M and Maskawa K 1973 *Prog. Theor. Phys.* **49** 652
- [53] Towner I S and Hardy J C 2008 *Phys. Rev. C* **77** 025501
- [54] Franzini P and Moulson M 2004 *Annu. Rev. Nucl. Part. Sci.* **56**
- [55] Cabibbo N, Swallow E and Winston R 2004 *Phys. Rev. Lett.* **92** 251803
- [56] Gamiz E *et al* 2005 *Phys. Rev. Lett.* **94** 011803
- [57] Leutwyler H and Roos M 1984 *Z. Phys. C* **25** 91
- [58] Ramsey-Musolf M J and Tulin S 2008 *Phys. Rep.* **456** 1
- [59] Počanić D *et al* 2004 *Phys. Rev. Lett.* **93** 181803
- [60] Hardy J C and Towner I S 2005 *Phys. Rev. Lett.* **94** 092502
- [61] Christenson J H, Cronin J W, Fitch V L and Turlay R 1964 *Phys. Rev. Lett.* **13** 138
- [62] Alavi-Harati A *et al* 1999 *Phys. Rev. Lett.* **83** 22
- [63] Fanti V *et al* 1999 *Phys. Lett. B* **465** 335
- [64] Aubert B *et al* 2002 *Phys. Rev. Lett.* **89** 201802
- [65] Abe K *et al* 2002 *Phys. Rev. D* **66** 071102R
- [66] Herczeg P 2005 *J. Res. Natl. Inst. Stand. Technol.* **110** 453
- [67] Huet P and Sather E 1995 *Phys. Rev. D* **51** 379
- [68] Ramsey-Musolf M J 2001 *Fundamental Physics with Pulsed Neutron Beams* ed C R Gould, G L Greene, F Plasil and W M Snow (Singapore: World Scientific)
- [69] Kirkby D and Nir Y 2008 *Phys. Lett. B* **667** 153
- [70] Herczeg P 2001 *Prog. Part. Nucl. Phys.* **46** 413
- [71] Drees M and Rauch M 2003 *Eur. Phys. J. C* **29** 573
- [72] Callan C G and Treiman S B 1967 *Phys. Rev.* **162** 1494
- [73] Ando S, McGovern J A and Sato T 2009 *Phys. Lett. B* **677** 109
- [74] Lising L J 1999 Time reversal invariance—a test in free neutron decay *PhD Thesis* University of California, Berkeley
- [75] Schneider M B *et al* 1983 *Phys. Rev. Lett.* **51** 1239
- [76] Huber R *et al* 2003 *Phys. Rev. Lett.* **90** 202301
- [77] Sromicki J, Allet M, Bodek K, Hajdas W, Lang J, Müller R, Navert S, Naviliat-Cuncic O and Zejma J 1996 *Phys. Rev. C* **53** 932
- [78] Schreckenbach K 1988 *J. Phys. G: Nucl. Phys.* **14** S391
- [79] Byrne J *et al* 1989 *Nucl. Instrum. Methods A* **284** 116
- [80] Byrne J *et al* 1990 *Phys. Rev. Lett.* **65** 289
- [81] Nico J S *et al* 2005 *Phys. Rev. C* **71** 055502
- [82] Mampe W, Ageron P, Bates C, Pendlebury J M and Steyerl A 1989 *Phys. Rev. Lett.* **63** 593
- [83] Arzumanov S *et al* 2000 *Phys. Lett. B* **483** 15

- [84] Paul W, Anton F, Paul L, Paul S and Mampe W 1989 *Z. Phys. C* **45** 25
- [85] Huffman P R *et al* 2001 *Nature* **403** 62
- [86] Dzhosyuk S N *et al* 2005 *J. Res. Natl. Inst. Stand. Technol.* **110** 339
- [87] Paul S 2009 arXiv:0902.0169v1
- [88] Schreckenbach K and Mampe W 1992 *J. Phys. G: Nucl. Phys.* **18** 1
- [89] Spivak P E 1988 *Zh. Eksp. Fiz.* **94** 1
- [90] Nezvizhevskii V V *et al* 1992 *JETP* **75** 405
- [91] Mampe W, Bondarenko L N, Morozov V I, Panin Y N and Fomin A I 1993 *JETP Lett.* **57** 82
- [92] Byrne J *et al* 1996 *Europhys. Lett.* **33** 187
- [93] Serebrov A P *et al* 2008 *Phys. Rev. C* **78** 035505
- [94] Abele H *et al* 2002 *Phys. Rev. Lett.* **88** 211801
- [95] Glück F *et al* 2005 *Eur. Phys. J. A* **23** 135
- [96] Wietfeldt F E *et al* 2005 *Nucl. Instrum. Methods A* **545** 181
- [97] Häse H *et al* 2002 *Nucl. Instrum. Methods A* **485** 453
- [98] Petoukhov A *et al* 2003 *Quark Mixing, CKM Unitarity* ed D Mund and H Abele (Heidelberg: Mattes Verlag)
- [99] Kreuz M *et al* 2005 *Nucl. Instrum. Methods A* **547** 583
- [100] Zimmer O *et al* 2000 *Nucl. Instrum. Methods A* **440** 764
- [101] Young A R *et al* 2001 *Fundamental Physics with Pulsed Neutron Beams* ed C R Gould, G L Greene, F Plasil and W M Snow (Singapore: World Scientific)
- [102] Martin J W *et al* 2003 *Phys. Rev. C* **68** 055503
- [103] Martin J W *et al* 2006 *Phys. Rev. C* **73** 015501
- [104] Pattie R W *et al* 2009 *Phys. Rev. Lett.* **102** 012301
- [105] Mostovoi Y A *et al* 2001 *Phys. At. Nuclei* **64** 1955
- [106] Carnoy A S *et al* 1992 *J. Phys. G: Nucl. Phys.* **18** 823
- [107] Kuznetsov I A *et al* 1995 *Phys. Rev. Lett.* **75** 794
- [108] Serebrov A P *et al* 1998 *JETP* **86** 1074
- [109] Schumann M *et al* 2007 *Phys. Rev. Lett.* **99** 191803
- [110] Kreuz M *et al* 2005 *Phys. Lett. B* **619** 263
- [111] Barenboim G, Bernabéu J, Prades J and Raidal M 1997 *Phys. Rev. C* **55** 4213
- [112] Abachi S *et al* 1996 *Phys. Rev. Lett.* **76** 3271
- [113] Profumo S, Ramsey-Musolf M J and Tulin S 2007 *Phys. Rev. D* **75** 075017
- [114] Glück F, Joó I and Last J 1995 *Nucl. Phys. A* **593** 125
- [115] Glück F 1996 *Phys. Lett. B* **376** 25
- [116] Sjue S K L 2005 *Phys. Rev. C* **72** 045501
- [117] Gudkov V 2008 *Phys. Rev. C* **77** 045502
- [118] Treiman S B 1958 *Phys. Rev.* **110** 448
- [119] Habeck C 1997 Experimental determination of the weak coupling constant ratio G_A/G_V in neutron decay
PhD Thesis University of Sussex
- [120] Schumann M *et al* 2008 *Phys. Rev. Lett.* **100** 151801
- [121] Wietfeldt F E 2005 *Mod. Phys. Lett. A* **20** 1783
- [122] Mostovoy Y and Frank A 1976 *JETP Lett.* **24** 38
- [123] Gardner S and Zhang C 2001 *Phys. Rev. Lett.* **86** 5666
- [124] Stratowa C, Dobrozemsky R and Weinzierl P 1978 *Phys. Rev. D* **18** 3970
- [125] Byrne J *et al* 2002 *J. Phys. G: Nucl. Part. Phys.* **28** 1325
- [126] Zimmer O, Byrne J, van der Grinten M G D, Heil W and Glück F 2000 *Nucl. Instrum. Methods A* **440** 543
- [127] Baeßler S *et al* 2008 *Eur. Phys. J. A* **38** 17
- [128] Yerozolimsky B 2004 arXiv:nucl-ex/0401014
- [129] Wilburn W S *et al* 2001 *Fundamental Physics with Pulsed Neutron Beams* ed C R Gould, G L Greene, F Plasil and W M Snow (Singapore: World Scientific)
- [130] Počanić D *et al* 2008 arXiv:0810.0251v1
- [131] Wenninger H, Steiwe J and Leutz H 1968 *Nucl. Phys. A* **109** 561
- [132] FRIB 2009 Facility For Rare Isotope Beams. www.er.doe.gov/np/program/FRIB.html
- [133] Lising L J *et al* 2000 *Phys. Rev. C* **62** 055501
- [134] Soldner T, Beck L, Plonka C, Schreckenbach K and Zimmer O 2004 *Phys. Lett. B* **581** 49
- [135] Calaprice F P 1985 *Hyperfine Interact.* **22** 83
- [136] Mumm H P *et al* 2004 *Rev. Sci. Instrum.* **75** 5343
- [137] Plonka C 2004 Untersuchung der Zeitumkehrinvarianz am D-Koeffizienten des freien Neutronenzerfalls mit TRINE *PhD Thesis* Technische Universität München

- [138] Gaponov Y V and Khafizov R U 2000 *Nucl. Instrum. Methods A* **440** 557
- [139] Beck M *et al* 2002 *JETP Lett.* **76** 332
- [140] Nico J S *et al* 2006 *Nature* **444** 1059
- [141] Fisher B M *et al* 2005 *J. Res. Natl. Inst. Stand. Technol.* **110** 421
- [142] Gentile T R *et al* 2007 *Nucl. Instrum. Meth. A* **570** 447
- [143] Cooper R L 2008 The radiative decay mode of the free neutron *PhD Thesis* University of Michigan
- [144] Kabir P K 1967 *Phys. Lett. B* **24** 601
- [145] Nemenov L L 1980 *Sov. J. Nucl. Phys.* **31** 1
- [146] Bryne J 2001 *Europhys. Lett.* **56** 633
- [147] Green K and Thompson D 1990 *J. Phys. G: Nucl. Phys.* **16** L75
- [148] Nemenov L L and Ovchinnikova A A 1980 *Sov. J. Nucl. Phys.* **31** 5
- [149] Schott W, Dollinger G, Faestermann T, Friedrich J, Hartmann F J, Hertenberger R, Kaiser N, Müller A R, Paul S and Ulrich A 2006 *Eur. Phys. J. A* **30** 603
- [150] Dubbers D *et al* 2008 *Nucl. Instrum. Methods A* **596** 238